Supplementary Online Material

General information about the Sungir burials and habitation site

The general results of excavations at Sungir, including stratigraphy, and lithic and bone assemblages, were published some decades ago (Bader 1978). However, the release of details for the burials and physical anthropology was significantly delayed. All the results of the investigation of Sungir have now been published (see Zubov 1984; Bader and Lavrushin 1998; Alekseeva and Bader 2000; Trinkaus et al. 2014; Vasilyev and Gerasimova 2017; Zhitenev 2017), including analysis of Paleolithic human DNA (Sikora et al. 2017).

Grave 1 (Fig. S1), besides the S-1 skeleton, contains numerous artifacts made of ivory and animal bones, and some lithics. There are ca. 20 thin ivory bracelets and several ivory bead bracelets on the male's hands, and several bone pendants. There is also a triple row of ivory beads on his head, and 20 drilled Arctic fox canines on its back. Ivory beads (ca. 3500) decorated the clothes, and this allowed reconstruction of the shape and size of the clothes. There were also rows of beads lying along the arms, legs and body, as well as across the chest and hip bones. As for the lithic artifacts, drilled pebbles on the chest, a flint knife, and a scraper were found.

Grave 2 (Fig. S2) contained the remains of two sub-adult males (S-2 and S-3) lying antithetically head to head. The burial was simultaneous, since large spears made of mammoth ivory were placed in the grave alongside the bodies. One of the main distinctive features of Grave 2 are two ivory spears (2.42 m and 1.66 m long) and 12 ivory javelins; two pendants in the form of a horse or saiga antelope, and bison; two large ivory pins; four antler shaft wrenches; 25 ivory bracelets and 13 bead bracelets on the hands; drilled pebbles; a large bone sculpture of a mammoth (S-2); slotted disks; three ivory daggers; four ivory finger rings; and a bone needle. Around 2730 ivory beads were sewn on to the clothes and headgear of S-2, and ca. 3500 beads on S-3.

Based on the large number of beads in graves 1 and 2 (in total, ca. 9730), and their arrangement in rows along arms, legs, across the skeleton, and above and below it, it is possible to assume that they were sewn on to clothes (Bader 1998; Gilligan 2019). For S-1, two layers of clothes can be established. The lower fitted garments were a fur or leather parka (a high-necked shirt, put on over the head), and trousers sewn with light moccasin-like shoes. The upper garment was a cloak-like piece. The headgear was decorated with bone beads and drilled Arctic fox canines. For S-2 and S-3, similar lower and upper garments were detected. The footwear of S-2 was reconstructed as high fur boots (*mukluks* type) tied above the knees. The headgears for S-2 and S-3 have richer ornaments compared to S-1: in addition to three rows of beads at the front and at the back, it has Arctic fox canines on its top and a small flat ring, perhaps for tying together Arctic fox tails on the headgear.

Based on analysis of some of the lithic artifacts from Sungir (ca. 2400 items, including 1624 tools of regular shape and 779 irregularly retouched/notched flakes and blades), it is possible to conclude that the stone tools belong to the following categories: burins; chisel-shaped tools (*pièce écailée*); chips with trimming; triangular and leaf-shaped points with bifacial and unifacial retouch; bifaces; points on flakes, blades and bladelets; borers; side scrapers (Fig. S3; Fig. S4: 11–18); backed knives; combined tools, and retouched blades and flakes. *Pièce écailée*, scrapers and burins are the most numerous kinds of tools, in addition to blades and retouched flakes. Among other tool types, important for cultural identification, are bifacial points (Fig. S4: 1–10); and scrapers and points made on blades and bladelets. The majority of blades and almost all flakes were manufactured by direct percussion. As for the raw materials, different varieties of boulder and pebble flint (the dominant kind of stone), and silicified limestone, quartz, quartzite and slate were used for tool manufacture.

Revision of the site's stratigraphy and spatial distribution of artifacts

The number of artifacts we entered into the database is ca. 64,890 (Fig. S12). Adtollo's Topocad and QGIS 3.14 computer packages were used. Unfortunately, the exact depths of artifacts were not originally measured during the excavations, because the cultural layer was divided by arbitrary levels/horizons (each 5–35 cm thick), and we followed this subdivision. The number of levels is from three to six in different parts of the site. The total thickness of a cultural layer, which contains the burials, is from ca. 30–40 cm to ca. 1 m. As for the parts of the site disturbed by quarrying to remove clay for the brick factory, practiced before the discovery of Sungir in 1955, we were able to reconstruct these areas, including those where a cultural layer was only partially preserved (Fig. S12).

A two-dimensional map of finds' density ("heat-map") was compiled for the first time (Fig. S12). It shows the concentrations of artifacts, bones, and other features (spots enriched in charcoal and ocher) in certain parts of site (notably, excavation pits II and III). The areas with the highest density of artifacts were preliminary considered to represent the dwellings.

For Pit II, where the burials were found, we were able to record in more detail the spatial distribution of different categories of finds, such as artifacts, concentrations of charcoal, red ocher, animal bones, and humic-enriched spots (Fig. S13). By doing this, we established for the first time the stratigraphic position of the level from which the burial pits were dug.

According to Bader (1978), the surface from which the grave pits were dug was marked by the S-5 skull in Grave 1. It was found 15 cm above the contact of the paleosol (essentially, the cultural layer) and the underlying sandy loam (bedrock). Thus, Bader (1978) assumed that the Sungir graves were dug from the lower part of the paleosol. After the publication of the monograph edited by Bader and Lavrushin (1998), Gavrilov (2001) suggested that the graves were dug from a higher stratigraphic level. The revision of O. N. Bader's field drawings made it possible for the first time to judge more accurately the stratigraphic position of the burials associated with the large concentration of ocher.

There are not many artifacts and other finds in the upper horizons of the grids where the graves were found (Figs. S12–S13), and immediately around them. Their number increases, but not significantly, with depth (Fig. S13). The spaces between the graves contain the smallest amount of finds in all horizons. Hearth pits between the burials, despite the fact that they were dug from different elevations (some from below the bedrock, and some above it), are still found only in Horizon 5 (Fig. S13).

Small particles of ocher were recorded in Horizon 2, starting from the level of 20–30 cm above the S-5 skull in Grave 1. Given that this skull was deposited on a bed of ocher, it is likely that the ocher spots above it mark the infill of the grave pit. In this case, the burial pit of S-1 was dug approximately from the second arbitrary level or the upper part of the paleosol. A similar picture emerges when analyzing the features of the cultural layer at the location of Grave 2. The traces of burials were recorded 3–5 cm below the contact of the paleosol and bedrock, at a depth of 78 cm from the top of the cultural layer. However, the first signs of this burial appeared much higher – also at the level of the second arbitrary level, in the form of a dark humus concentration of irregular shape with the inclusion of ocher spots. This feature has the same orientation as Grave 2: from southwest to northeast. Concentrations of ocher and humic-enriched spots, and bones are located above the graves 1–2.

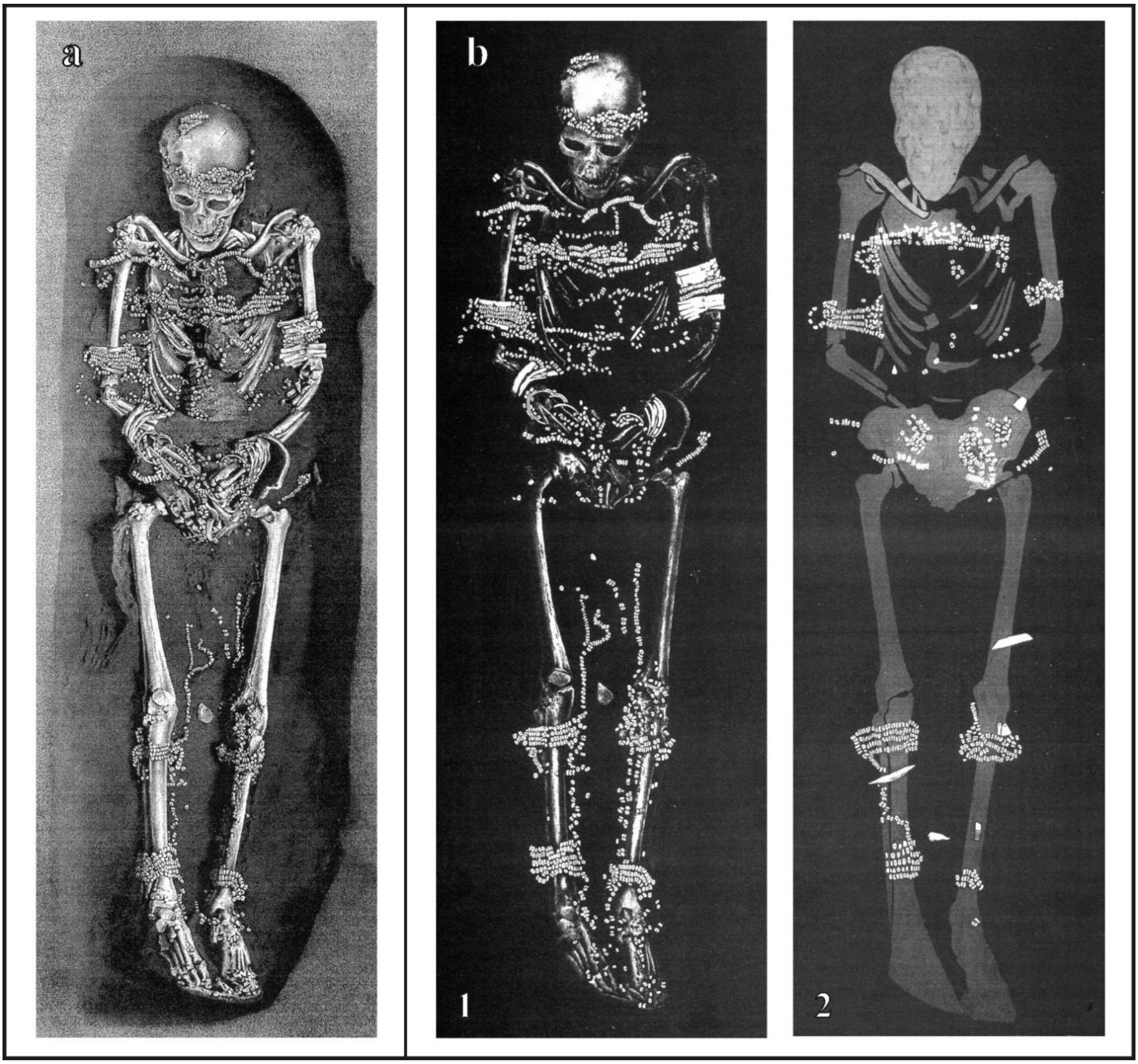

Fig. S1. The Sungir-1 burial: a – general view; b – location of beads and other adornments (1 – on the skeleton; 2 – beneath the skeleton) (after Bader 1998; modified).

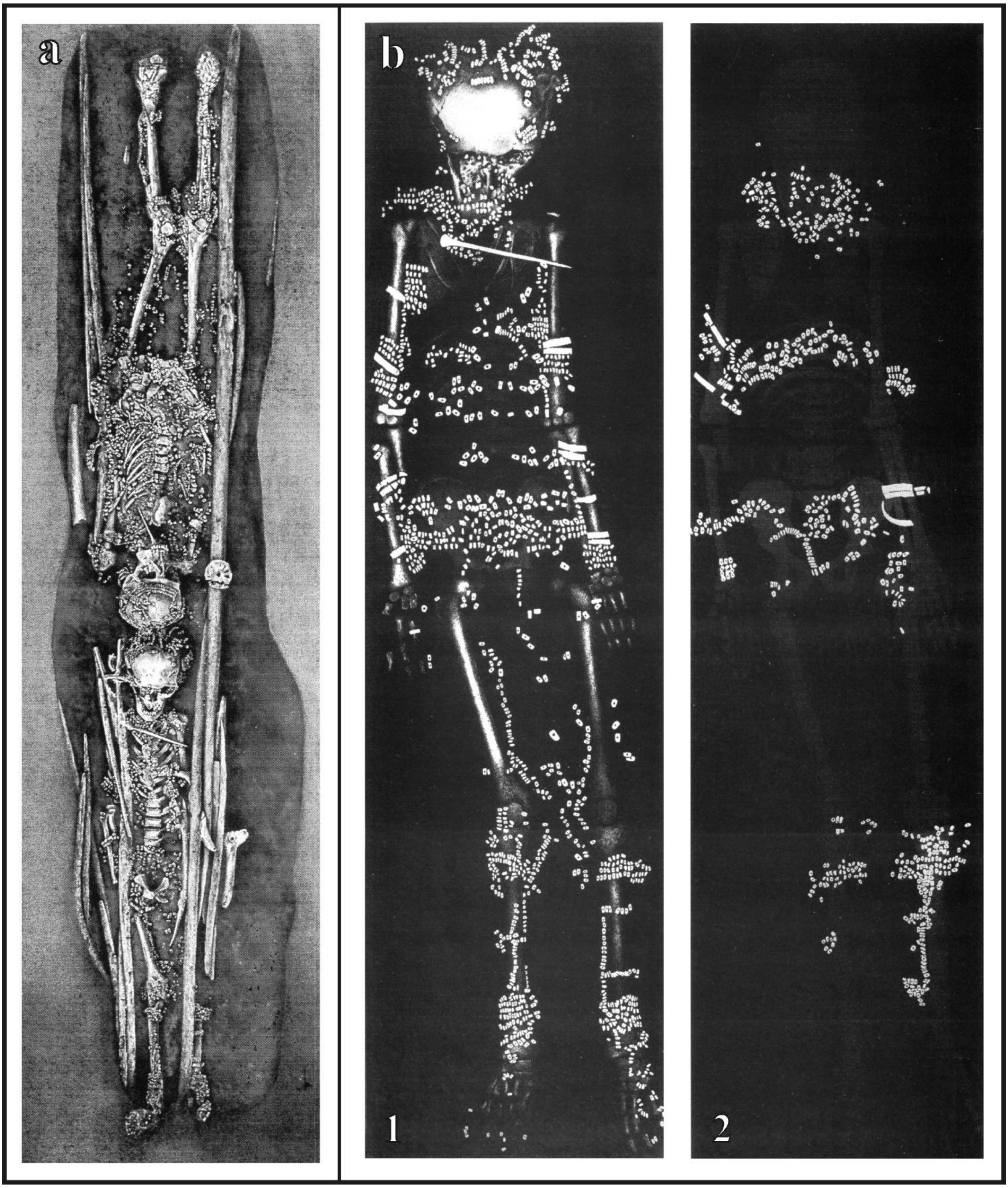

Fig. S2. The double burial of Sungir-2 and Sungir-3: a – general view (Sungir-2 is below, and Sungir-3 is above); b – location of beads and other adornments on Sungir-2 (1 – on the skeleton; 2 – beneath the skeleton) (after Bader 1998; modified).

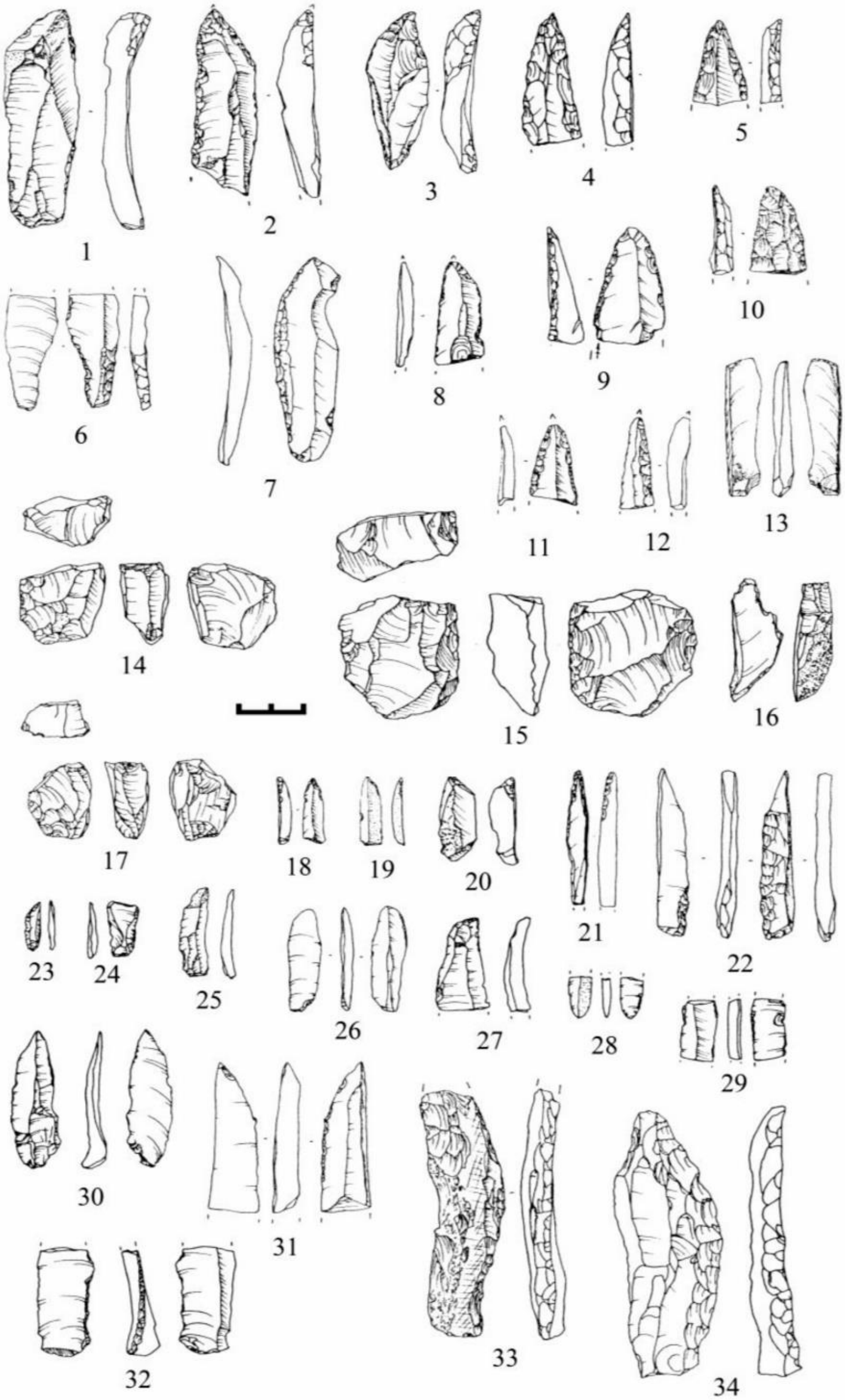

Fig. S3. Lithic artifacts from the Sungir site: points on blades (1–5, 7–12, 30–31), fragment of tanged point (6), burin spalls (13, 16, 21, 22), edge-faceted cores for bladelets (14, 17), preform of edge-faceted core for bladelets (15), points on bladelets (18–20, 23), bladelets (24–25, 27, 29), retouched bladelets (26, 28), retouched blades (32–33), and borer (34) (after Gavrilov 2017; modified).

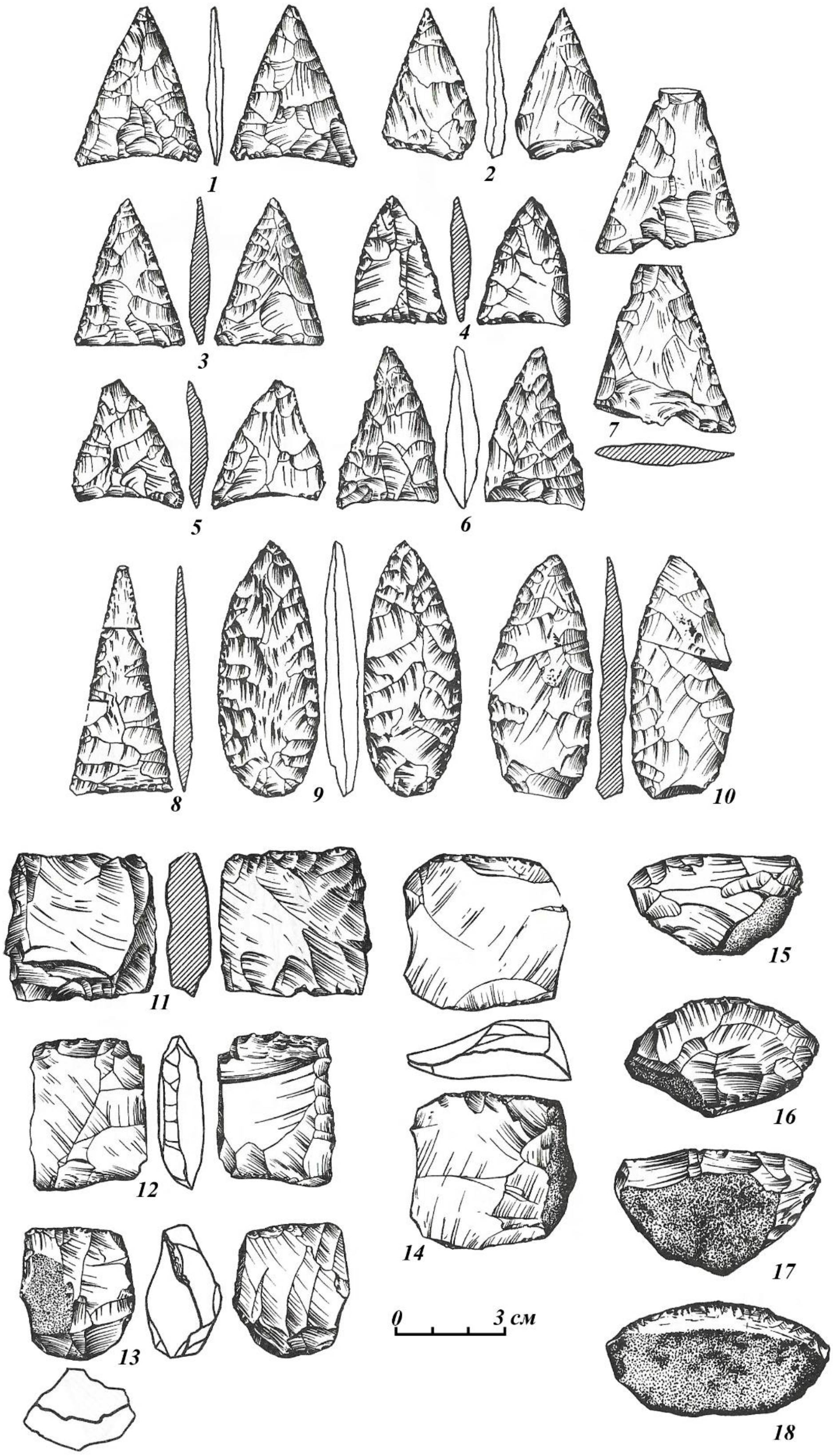

Fig. S4. Lithic artifacts from the Sungir site: 1–10 – bifacial points; 11–14 – *pièce écailée*; 15–18 – side scrapers (after Bader 1978; modified).

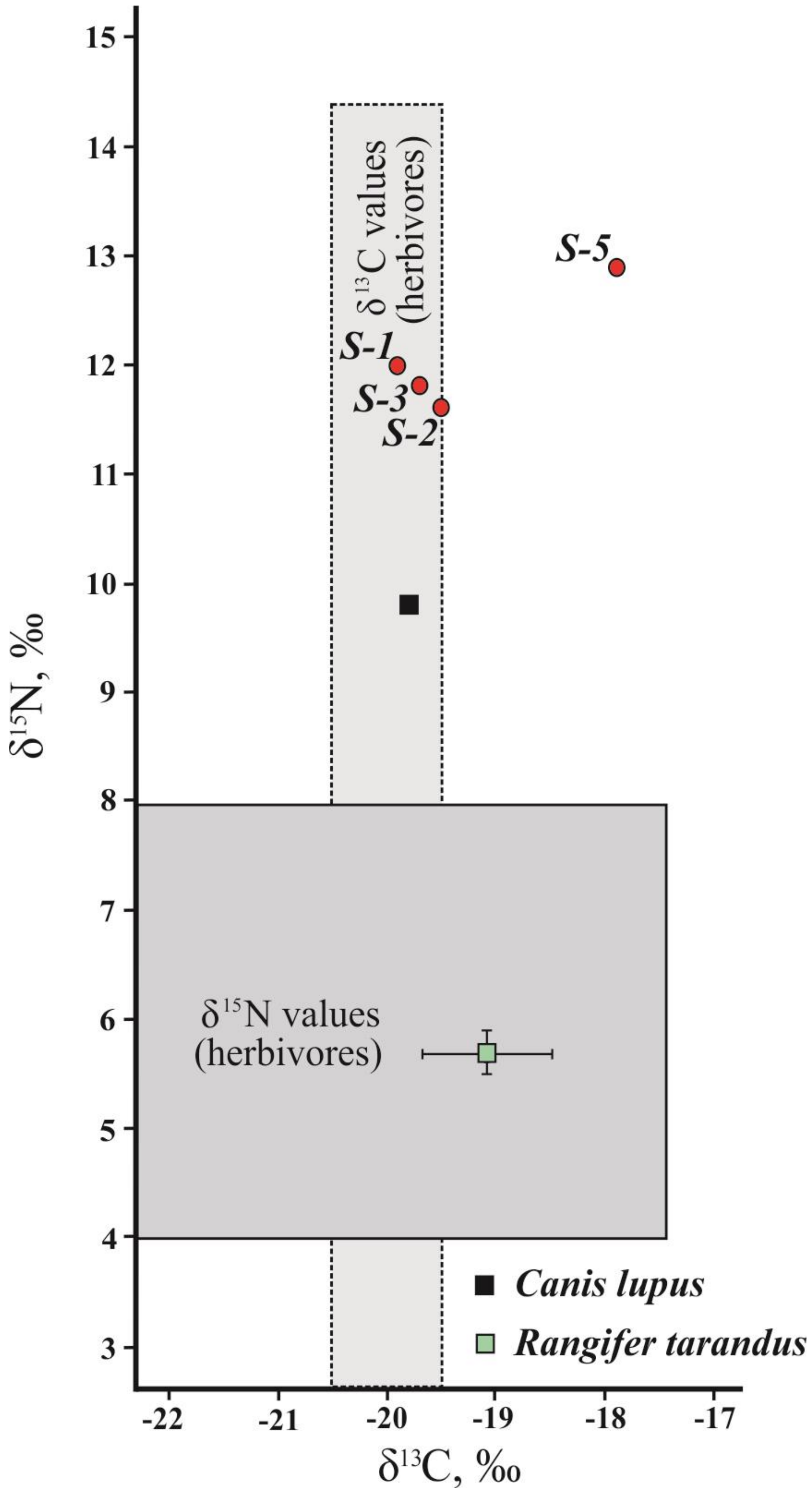

Fig. S5. The stable isotope composition of the Sungir humans in relation to animals from the Sungir. Average value for reindeer are plotted with ± 2 s.d. (Trinkaus et al. 2014); the gray rectangles show the variations for $\delta^{13}C$ and $\delta^{15}N$ of terrestrial herbivores' collagen (Richard and Trinkaus 2009).

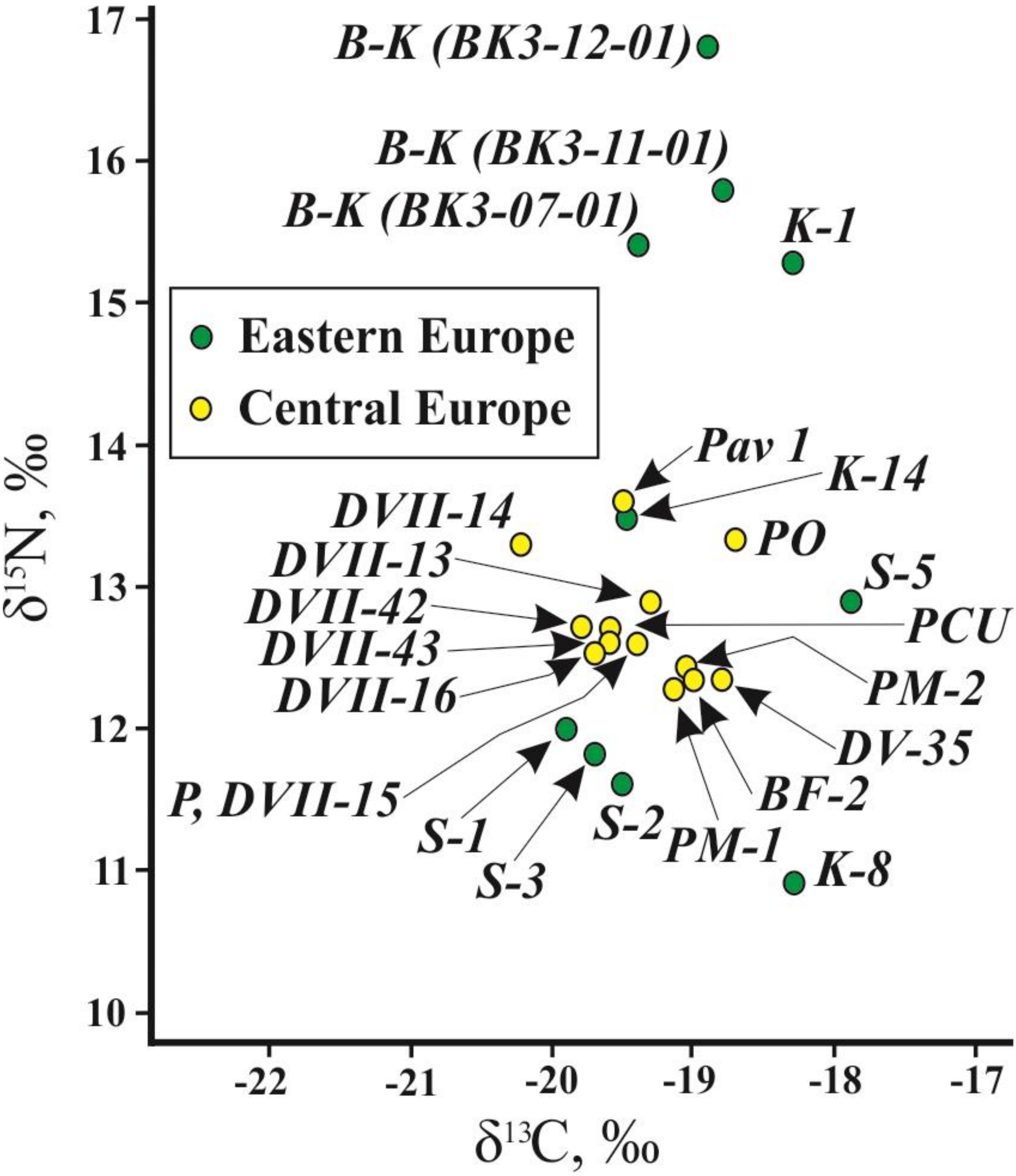

Fig. S6. Comparison of $\delta^{13}C$ and $\delta^{15}N$ values for Early Upper Paleolithic humans from Eastern and Central Europe (see Table S2; for S-1–S-3 individuals, values from this paper are used). Abbreviations: BK – Buran-Kaya III (different individuals); K-1 – Kostenki 1; K-14 – Kostenki 14; K-8 – Kostenki 8; S-1 – Sungir, S-1; S-2 – Sungir, S-2; S-3 – Sungir, S-3; S-5 – Sungir, S-5; PO – Peştera cu Oase 1; PCU – Peştera Cioclovina Uscată 1; P – Předmostí 1; PM-1 – Peştera Muierii 1; PM-2 – Peştera Muierii 2; BF-2 – Brno-Francouzská 2; DV-35 – Dolní Věstonice 35; Pav – Pavlov; DVII13–43 – Dolní Věstonice II (different individuals).

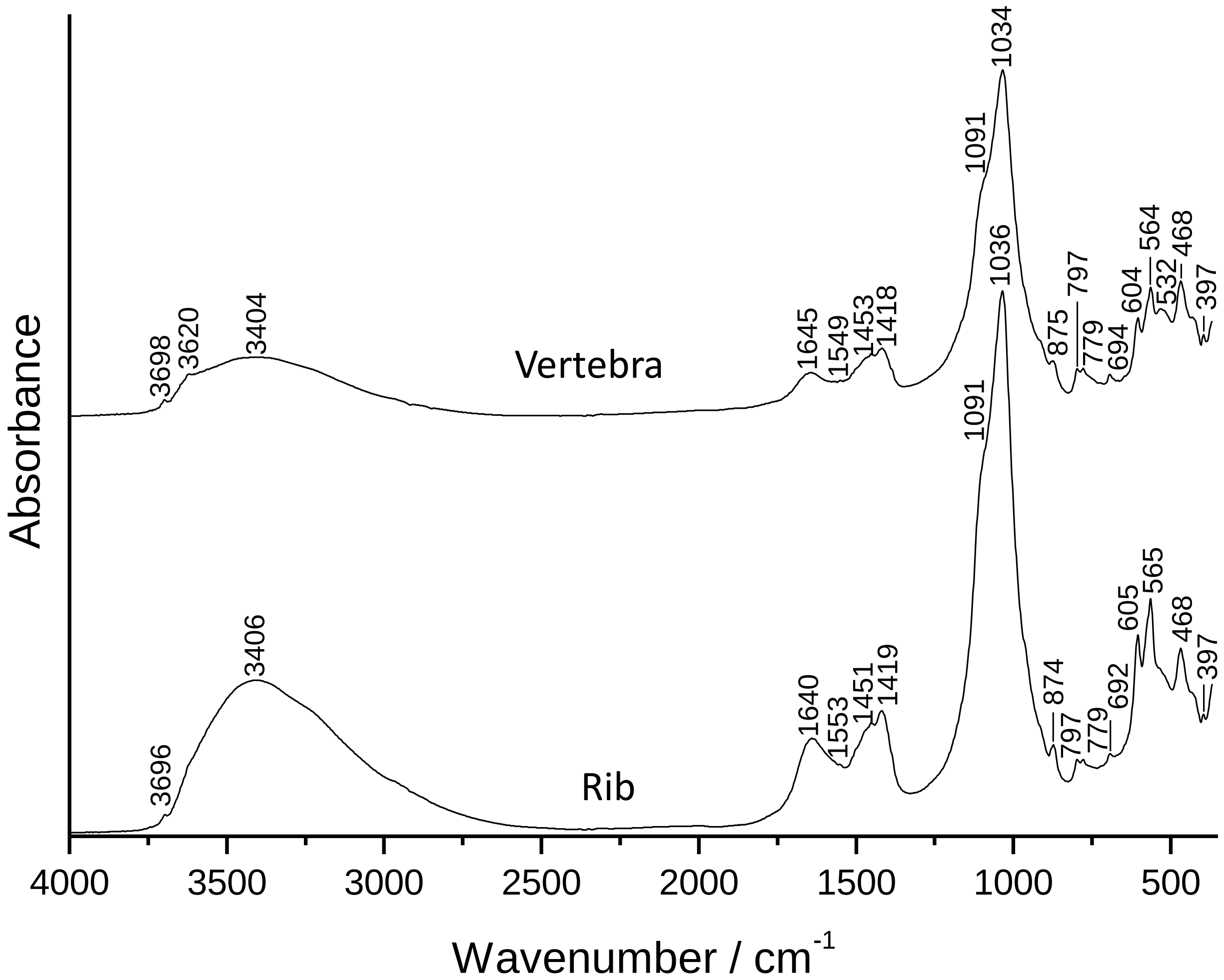

Wavenumber (cm^{-1})	Attribution
397	Quartz, ν_sSiO, E mode
468	$\nu_2PO_4^{3-}$ and/or silicates
532	Clay
564-5	$\nu_{as4}PO_3^{4-}$
604-5	$\nu_{as4}PO_3^{4-}$
692-4	Quartz, ν_sSiO, E mode
779	Quartz, ν_sSiO, A_2 mode
797	Quartz, ν_sSiO, E mode
874-5	$\nu_2CO_3^{2-}$
1034-6	$\nu_3PO_3^{4-}$
1091	νPO_3^{4-}
1418	$\nu_3CO_3^{2-}$
1451-3	
1549-53	Amide II - νN-H, νC-N (collagen)
1640-45	Amide I - νC=O and/or OH deformation of water
3339-3461	νOH
3620	νOH clay
3696-8	νOH clay

Fig. S7. FTIR spectra of the bone surface of two bones of Sungir-1 skeleton and attributions of the respective vibrational bands in the table (ν: stretching vibration; as: asymmetric; s: symmetric). The extracted collagen from the vertebra corresponds to RICH-27986.1.1 and RICH-27986.2.1 (two extractions were performed on different parts of the bone) and the extracted collagen from the rib corresponds to RICH-27985.1.1 and RICH-27985.2.1 (two extractions were also performed on different parts of the bone).

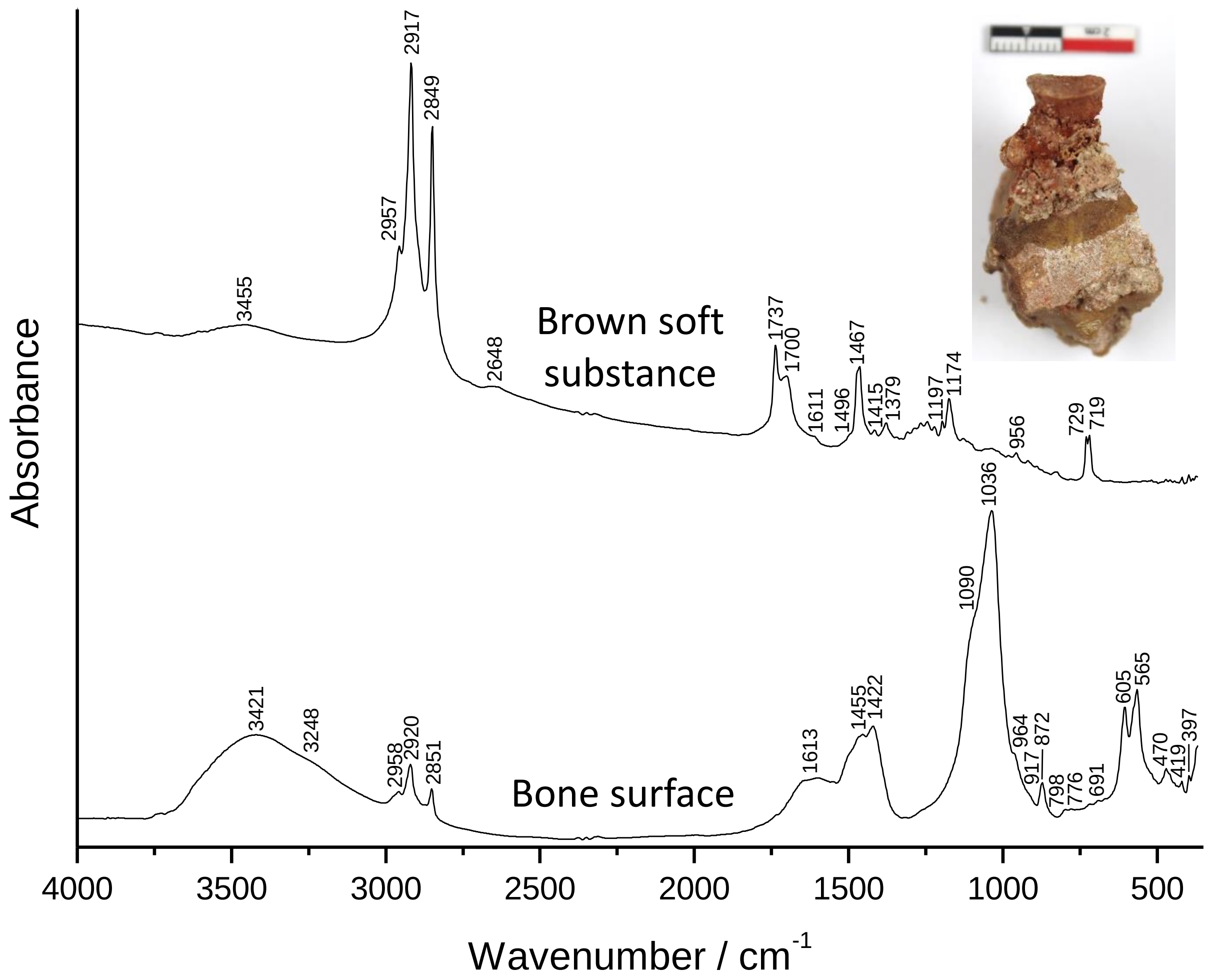

Wavenumber (cm^{-1})	Attribution
397	Quartz, v_sSiO, E mode
419	Silicates
470	$v_2PO_4^{3-}$ &/or silicates
565	$v_{as4}PO_3^{4-}$
605	$v_{as4}PO_3^{4-}$
691	Quartz, v_sSiO, E mode
719	Beeswax
729	Beeswax
776	Quartz, v_sSiO, A_2 mode
798	Quartz, v_sSiO, E mode
872	$v_2CO_3^{2-}$
917	Clay
956	Beeswax
964	$v_1PO_4^{3-}$ (Hap)
1036	$v_3PO_4^{4-}$ & silicates
1090	vPO_3 & silicates
1174	Beeswax
1197	Beeswax
1379	Beeswax

Wavenumber (cm^{-1})	Attribution
1415	Beeswax
1422	vCO_3^{2-}
1455	
1467	Beeswax
1496	Beeswax
1611	Beeswax
1613	OH deformation of water
1700	Beeswax
1737	Beeswax
2648	Beeswax
2849	Beeswax
2917	Beeswax
2920	vCH (collagen + beeswax)
2957	Beeswax
2958	$v_{as}CH_2$ (collagen)
3248	vOH
3421	vOH
3455	Beeswax

Fig. S8. FTIR spectra of the bone (vertebra) surface of the Sungir-2 skeleton and of the soft brown surface consolidation (see picture) with attributions of the respective vibrational bands in the table (v: stretching vibration; as: asymmetric; s: symmetric). The collagen extracted from this bone corresponds to the RICH-30584.1.1 and the XAD from this bone is MUSE21173.

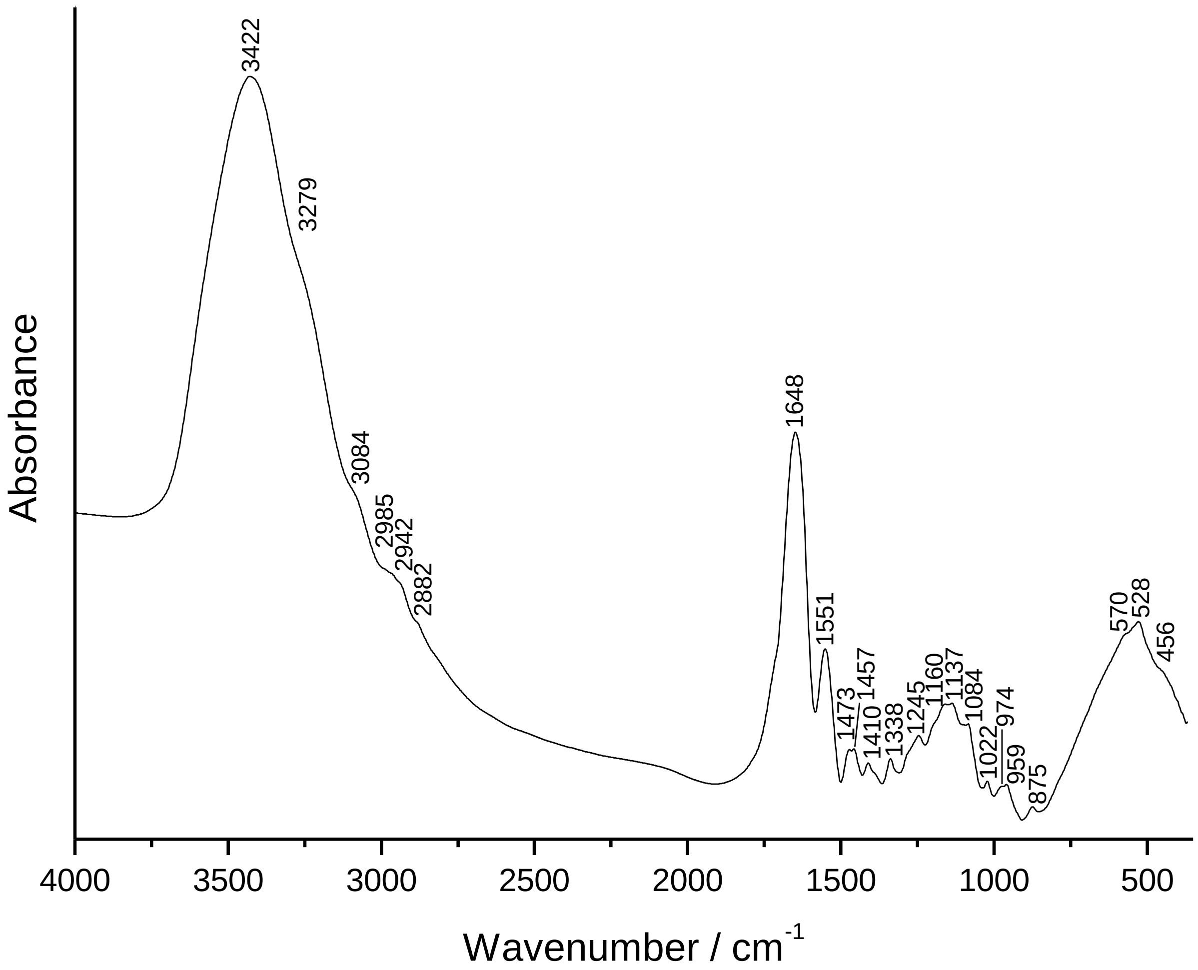

Sample ID	%C	%N	δ13C (‰)	δ15N (‰)	C/N	age (BP)	± (BP)	% collagen
RICH-30584.1.1	24.4	8.44	-20.0	11.8	3.4	21.788	120	6.35

Wavenumber (cm^{-1})	Attribution
456 (sh)	?
528	?
570	Phosphate
875	νC–C and νC-N
959	Polyvinyl Acetate, CH_3 wagging
974	νC–C or νC-O
1022	Polyvinyl acetate?
1084	νC-O
1137	Polyvinyl Acetate, νC-O and νC-C
1160	νC-O
1245	Amide III- νC-N, δN-H (collagen)
1338	CH_2 wagging (collagen - proline)
1410	
1457	CH_2 bending
1473	Deformation C-H
1551	Amide II - νN-H, νC-N (collagen)
1648	Amide I - νC=O and/or OH deformation of water
2882	νCH
2942	
2985	
3084	Amide B
3279	νOH/NH Amide A
3422	νOH Amide A

Fig. S9. FTIR spectrum of the collagen extracted from the bone (vertebra) surface of the Sungir-2 skeleton presenting soft brown substance consolidation with attributions of the respective vibrational bands in the table (ν: stretching vibration; as: asymmetric; s: symmetric).

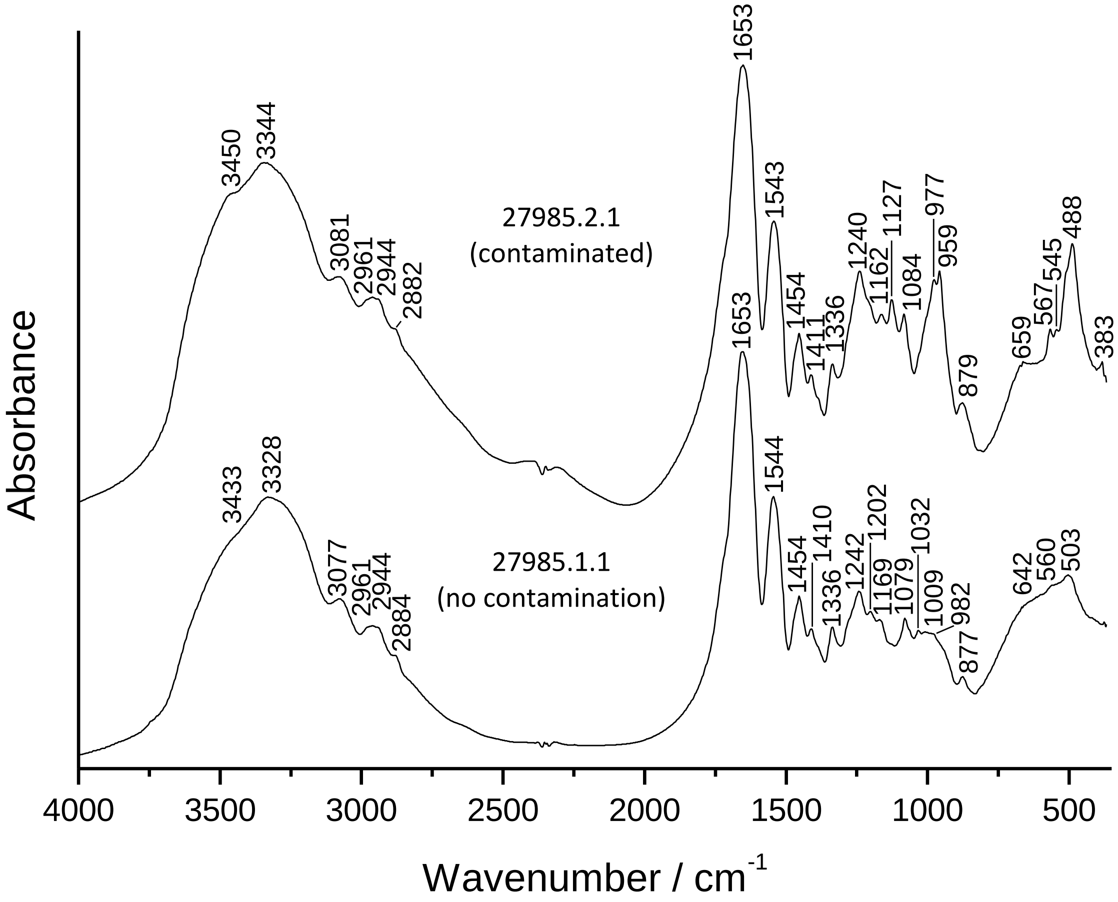

Wavenumber (cm^{-1})	Attribution
383	Phosphate
488	Phosphate
503	Amide V
560	NH out of plane bending
567	Phosphate
642-59	OH group/Amide IV (C=O)/aromatic ring Tyr
877-9	vC–C and vC-N
959	Polyvinyl Acetate, CH_3 wagging
977	Phosphate
1079-84	vC-O (collagen)
1127	vC-O (polyvinyl acetate)
1162-9	vC-O (collagen)
1202	Glycine and proline in collagen
1240-2	Amide III- vC-N, δN-H (collagen)
1336	CH_2 wagging (collagen - proline)
1410-1	
1454	CH_2 bending
1543-4	Amide II - vN-H, vC-N (collagen)
1653	Amide I - vC=O and/or OH deformation of water
2882-4	v_sCH aliphatic CH_x
2944	$v_{as}CH_2$ (collagen)
2961	
3077-81	Amide B
3228-344	vOH /NH Amide A
3433-50	vOH Amide A

Sample ID	%C	%N	$\delta^{13}C$ (‰)	$\delta^{15}N$ (‰)	C/N	age (BP)	± (BP)	% collagen
RICH-27985.1.1	29.64	10.60	-19.9	12.0	3.3	26.100	203	4,4
RICH-27985.2.1	28.84	10.05	-19.8	11.8	3.3	24.640	171	5.0

Fig. S10. The FTIR spectra of the collagens (two different extractions) extracted from the Sungir-1 skeleton (RICH-27985 – rib), with the attributions of the respective vibrational bands; in the table on the right the tabs highlighted in yellow show the bands of the contaminant (ν: stretching vibration; δ: bending vibration; as: asymmetric; s: symmetric; Tyr: tyrosine) and radiocarbon results in the table at the bottom (y: year).

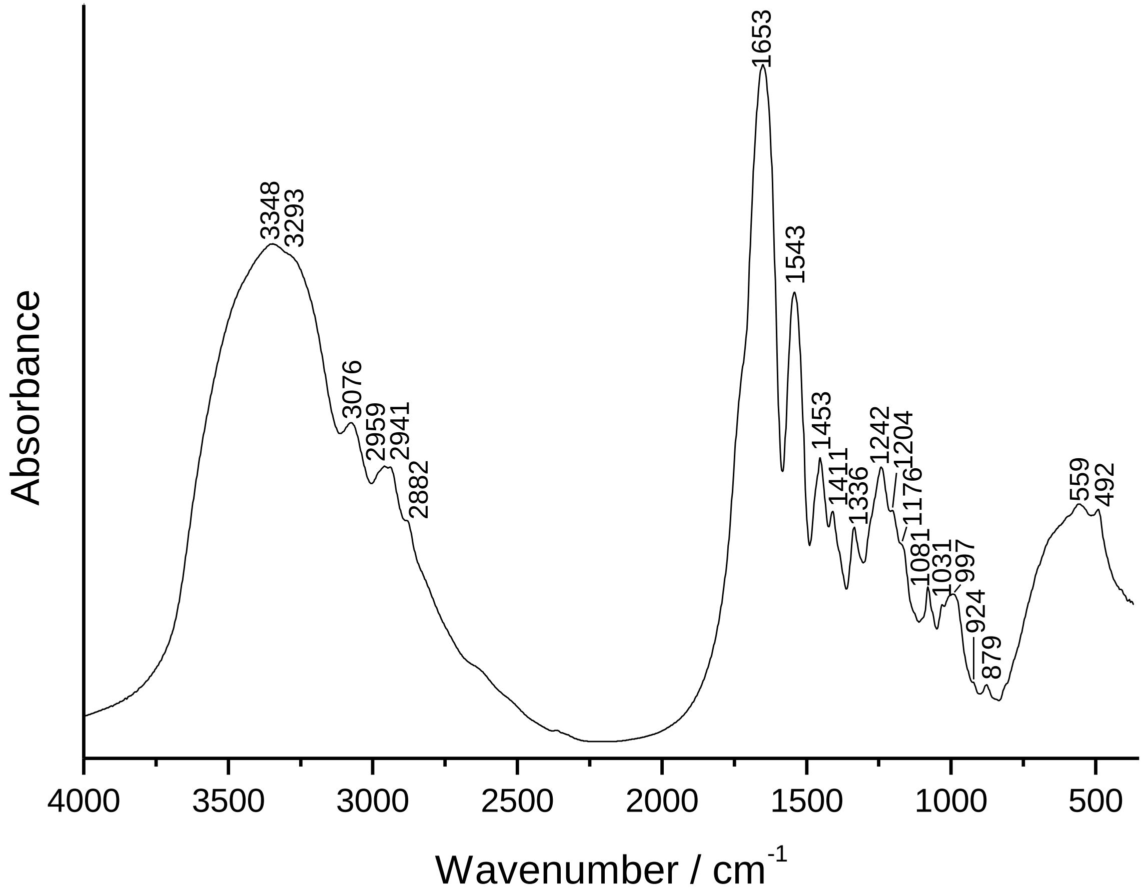

Wavenumber (cm^{-1})	Attribution
492	Amide V
559	NH out of plane bending
879	νC–C and νC-N
924	ρCH_2
997	νC–C or νC-O
1031	ν_{C-O} (collagen)
1081	
1176	
1204	Glycine and proline in collagen
1242	Amide III - νC-N, δN-H (collagen)
1336	CH_2 wagging (collagen - proline)
1411	
1453	CH_2 bending
1544	Amide II - νN-H, νC-N (collagen)
1653	Amide I - νC=O and/or OH deformation of water
2882	ν_sCH aliphatic CH_x
2941	$\nu_{as}CH_2$ (collagen)
2959	
3076	Amide B
3293	νOH/NH Amide A
3348	νOH Amide A

Sample ID	%C	%N	$\delta^{13}C$ (‰)	$\delta^{15}N$ (‰)	C/N	age (BP)	± (BP)	% collagen
RICH-27484.1.1	39.5	13.9	-19.5	11.6	3,3	25.906	130	15.1

Fig. S11. FTIR spectrum of the collagen extracted from the Sungir-2 skeleton (rib) with the attributions of the respective vibrational bands in the table on the right (ν: stretching vibration; δ: bending vibration; ρ: rocking; as: asymmetric; s: symmetric) and radiocarbon results in the table at the bottom.

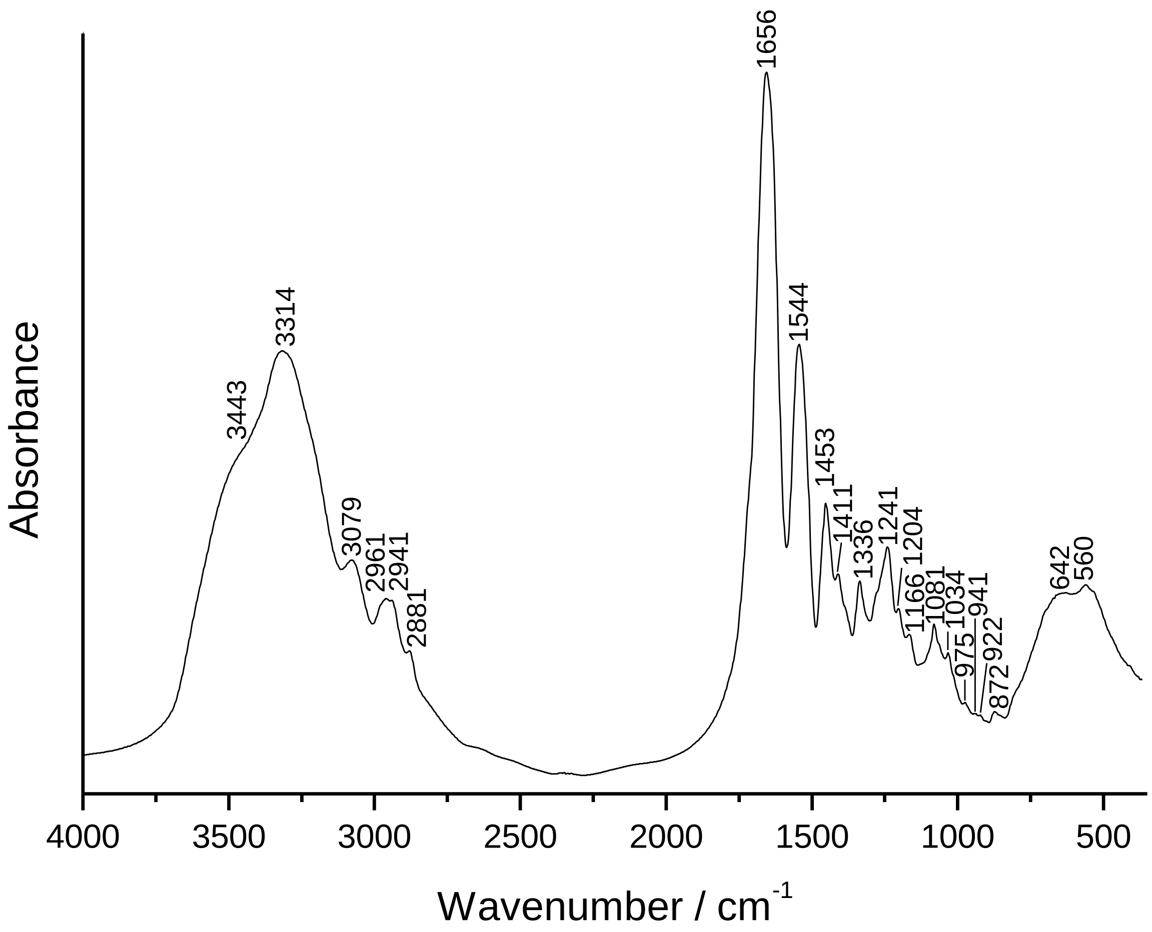

Sample ID	%C	%N	δ13C (‰)	δ15N (‰)	C/N	age (BP)	± (BP)	% collagen
RICH-27485.1.1	31,4	11,1	-19,7	11,8	3,3	26.784	143	9.1

Wavenumber (cm^{-1})	Attribution
560	NH out of plane bending
642	OH group/Amide IV (C=O)/aromatic ring Tyr
872	νC–C and νC-N
922	ρCH_2
941	
975	νC–C or νC-O
1034	ν_{C-O} collagen
1081	
1166	
1204	Glycine and proline in collagen
1241	Amide III- νC-N, δN-H (collagen)
1336	CH_2 wagging (collagen - proline)
1411	
1453	CH_2 bending
1544	Amide II - νN-H, νC-N (collagen)
1656	Amide I - νC=O and/or OH deformation of water
2881	ν_sCH aliphatic CH_x
2941	$\nu_{as}CH_2$ (collagen)
2961	
3079	Amide B
3314	νOH/NH Amide A
3443	νOH Amide A

Fig. S12. FTIR spectrum of the collagen extracted from the Sungir-3 skeleton (rib) with the attributions of the respective vibrational bands in the table on the right (ν: stretching vibration; δ: bending vibration; ρ: rocking; as: asymmetric; s: symmetric) and radiocarbon results in the table at the bottom.

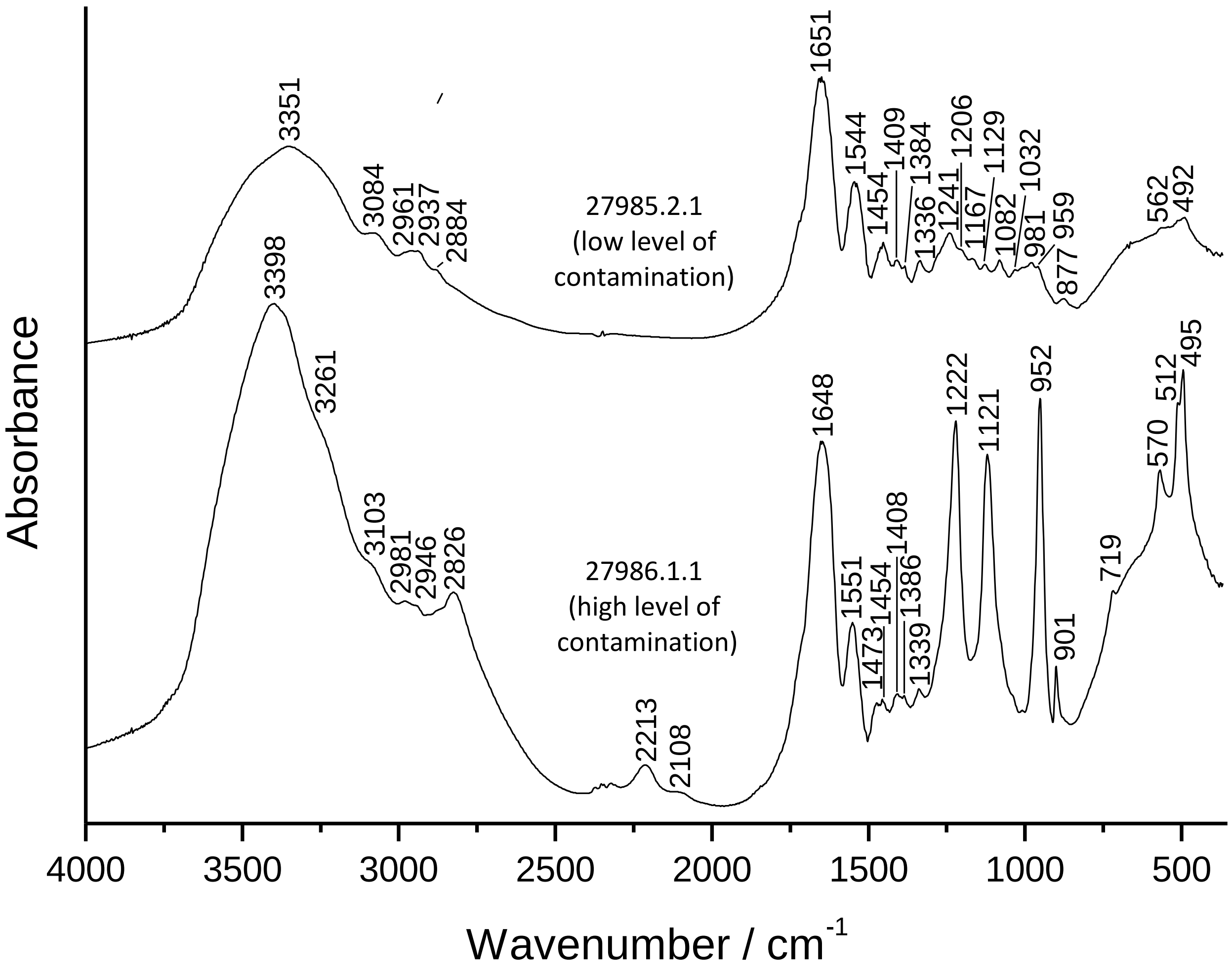

Sample ID	%C	%N	δ13C (‰)	δ15N (‰)	C/N	age (BP)	± (BP)	% collagen
RICH-27986.1.1	13.03	4.43	-20.4	12.1	3.4	19.751	107	5.4
RICH-27986.2.1	27.28	9.82	-19.8	12.0	3.2	25.500	189	3.7

Wavenumber (cm^{-1})	Attribution
492	Amide V
495	Phosphate
512	Phosphate
562	NH out of plane bending
570	Phosphate
719	Torsion C-H
877	vC–C and vC-N
901	Phosphate
952-9	Polyvinyl Acetate, CH_3 wagging
981	vC–C or vC-O
1032	vC-O (collagen)
1082	
1121-29	Polyvinyl Acetate, vC-O
1167	v_{C-O} (collagen)
1206	Glycine and proline in collagen
1222	Polyvinyl Acetate (PVAc), vC-O and vC-C
1241	Amide III- vC-N, δN-H (collagen)
1336-9	CH_2 wagging (collagen - proline)
1408-9	
1454	CH_2 bending
1473	Deformation C-H
1544-51	Amide II - vN-H, vC-N (collagen)
1648-51	Amide I - vC=O and/or OH deformation of water
2108	Phosphate
2213	
2826	vCH
2884	v_sCH aliphatic CH_x
2937-46	$v_{as}CH_2$ (collagen)
2961	
2981	vCH (Polyvinyl Acetate)
3084	Amide B
3103	vCH
3261	vOH
3351	vOH /NH Amide A
3398	vOH

Fig. S13. FTIR spectrum of the collagen extracted from the Sungir-1 skeleton (vertebra) with the attributions of the respective vibrational bands in the table on the right (ν: stretching vibration; δ: bending vibration; ρ: rocking; as: asymmetric; s: symmetric) and radiocarbon results in the table at the bottom.

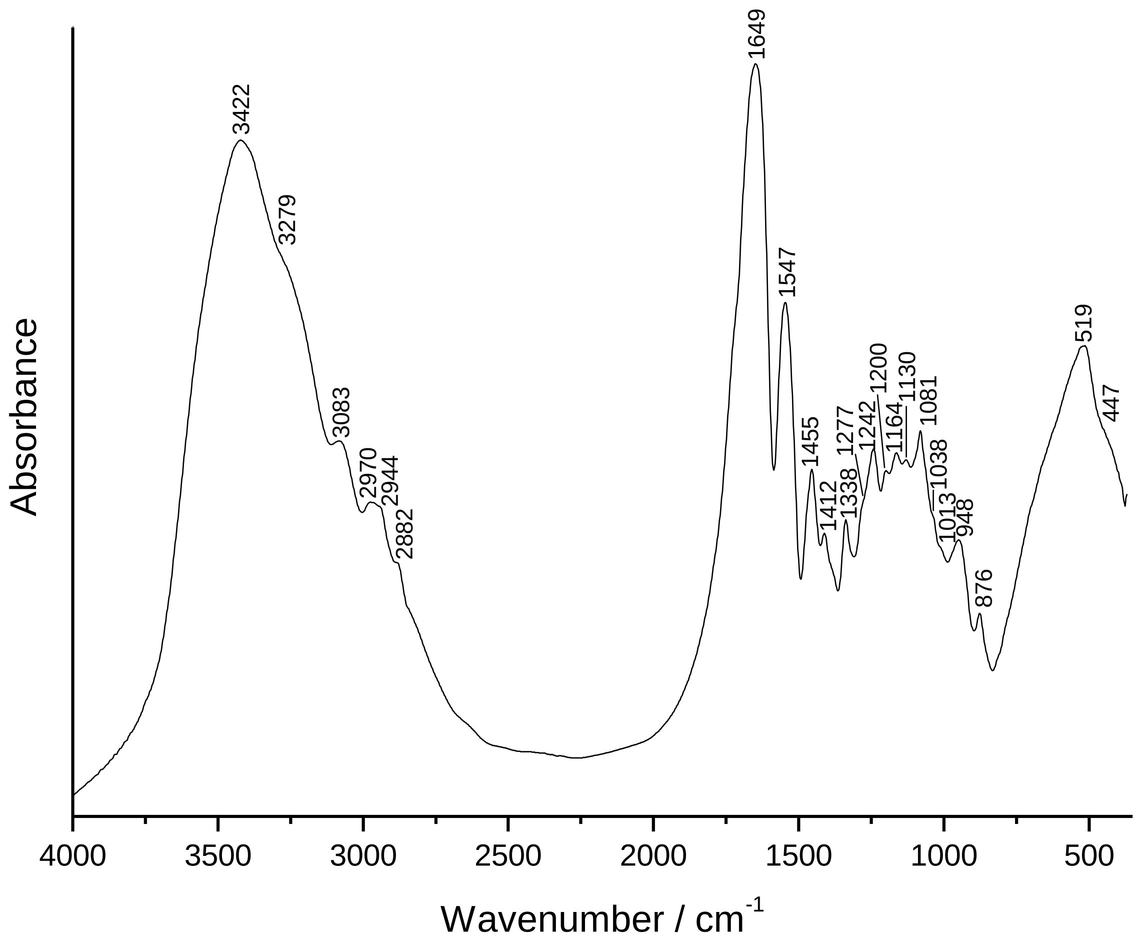

Sample ID	%C	%N	δ^{13}C (‰)	δ^{15}N (‰)	C/N	age (BP)	± (BP)	% collagen
RICH-30583.1.1	30.4	10.9	-19.6	12.1	3.3	25.532	179	7.55

Wavenumber (cm^{-1})	Attribution
447 (sh)	?
519	?
872	vC–C and vC-N
948	ρCH$_2$ (collagen) and/or Polyvinyl Acetate
1013 (sh)	Polyvinyl Acetate
1038	vC-O (collagen)
1081	
1130	Polyvinyl Acetate, vC-O
1164	vC-O (collagen)
1200	Glycine and proline in collagen
1242	Amide III- vC-N, δN-H (collagen)
1277 (sh)	?
1338	CH$_2$ wagging (collagen - proline)
1412	
1455	CH$_2$ bending
1547	Amide II - vN-H, vC-N (collagen)
1649	Amide I - vC=O and/or OH deformation of water
2882	v$_s$CH aliphatic CH$_x$
2944	v$_{as}$CH$_2$ (collagen)
2970	
3083	Amide B
3279	vOH/NH Amide A
3422	vOH Amide A

Fig. S14. FTIR spectrum of the collagen extracted from the Sungir-1 skeleton (other vertebra) with the attributions of the respective vibrational bands in the table on the right (ν: stretching vibration; δ: bending vibration; ρ: rocking; as: asymmetric; s: symmetric) and radiocarbon results in the table at the bottom.

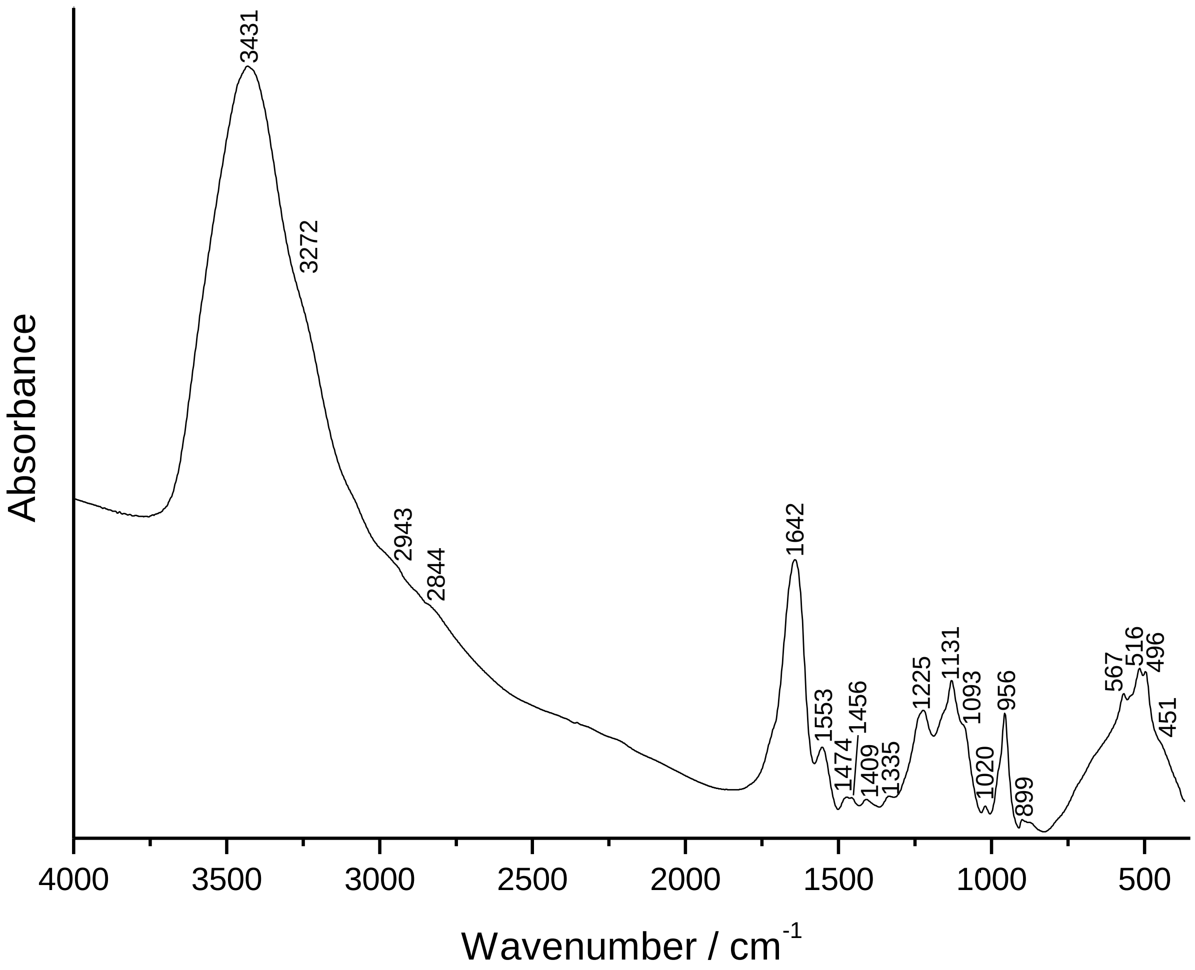

Wavenumber (cm^{-1})	Attribution
451 (sh)	
496	Phosphate
516	Polyvinyl Acetate? Phosphate?
567	Phosphate
899	Phosphate
956	Poly Vinyl Acetate, CH_3 wagging
1020	Polyvinyl Acetate?
1093 (sh)	νC-O
1131	Polyvinyl Acetate
1225	Polyvinyl Acetate, νC-O and νC-C
1335	CH_2 wagging (collagen - proline)
1409	
1456	CH_2 bending
1474	Deformation C-H
1553	Amide II - νN-H, νC-N (collagen)
1642	Amide I - νC=O and/or OH deformation of water
2844	νCH (polyvinyl acetate)
2943	$\nu_{as}CH_2$ (collagen)
3272	νOH
3431	

Sample ID	%C	%N	$\delta^{13}C$ (‰)	$\delta^{15}N$ (‰)	C/N	age (BP)	± (BP)	% collagen
RICH-30793.1.1	10.2	3.27	-20.9	11.5	3.7	15.244	64	3.57

Fig. S15. FTIR spectrum of the collagen extracted from the Sungir-1 skeleton (other piece of vertebra – same than RICH-30583) with the attributions of the respective vibrational bands in the table on the right (ν: stretching vibration; δ: bending vibration; ρ: rocking; as: asymmetric; s: symmetric) and radiocarbon results in the table at the bottom.

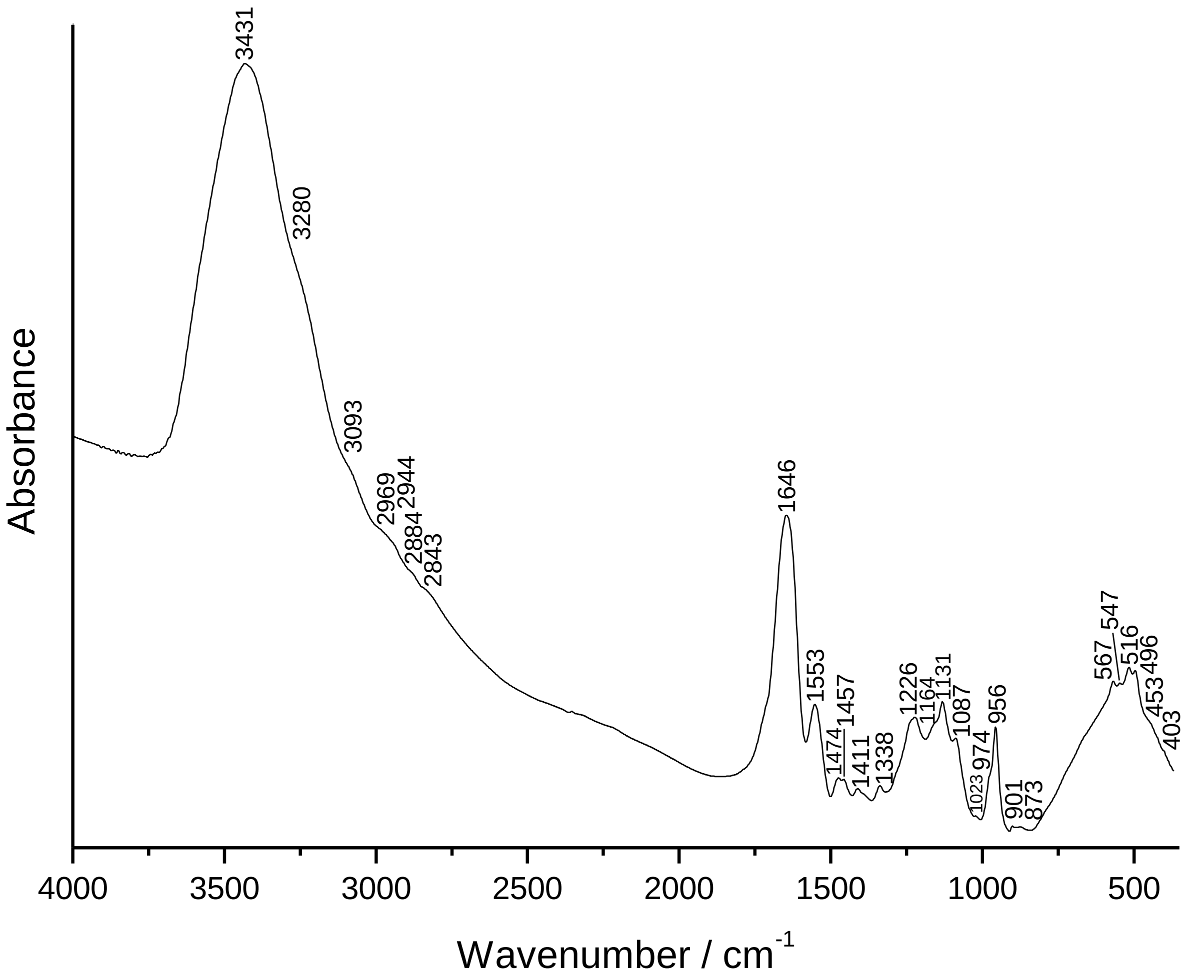

Sample ID	%C	%N	$\delta^{13}C$ (‰)	$\delta^{15}N$ (‰)	C/N	age (BP)	+-(BP)	% collagen
RICH-30585.1.1	14.1	4.97	-19.9	11.5	3.3	24.931	170	6.61

Wavenumber (cm^{-1})	Attribution
403	?
453 (sh)	?
496	Phosphate
516	Phosphate
547	?
567	Phosphate
873	νC–C and νC-N
901	Phosphate
956	Polyvinyl Acetate, CH_3 wagging
974	νC–C or νC-O
1023	Polyvinyl Acetate?
1087	νC-O
1131	Polyvinyl Acetate, νC-O
1164	νC-O
1226	Polyvinyl Acetate, νC-O and νC-C
1226	Amide III- νC-N, δN-H (collagen)
1338	CH_2 wagging (collagen - proline)
1411	
1457	CH_2 bending
1474	Deformation C-H
1553	Amide II - νN-H, νC-N (collagen)
1646	Amide I - νC=O and/or OH deformation of water
2843	νCH
2884	
2944	
2969	
3093	Amide B
3280	νOH/NH Amide A
3431	νOH Amide A

Fig. S16. FTIR spectrum of the collagen extracted from the Sungir-3 skeleton (vertebra) with the attributions of the respective vibrational bands in the table on the right (ν: stretching vibration; δ: bending vibration; ρ: rocking; as: asymmetric; s: symmetric) and radiocarbon results in the table at the bottom.

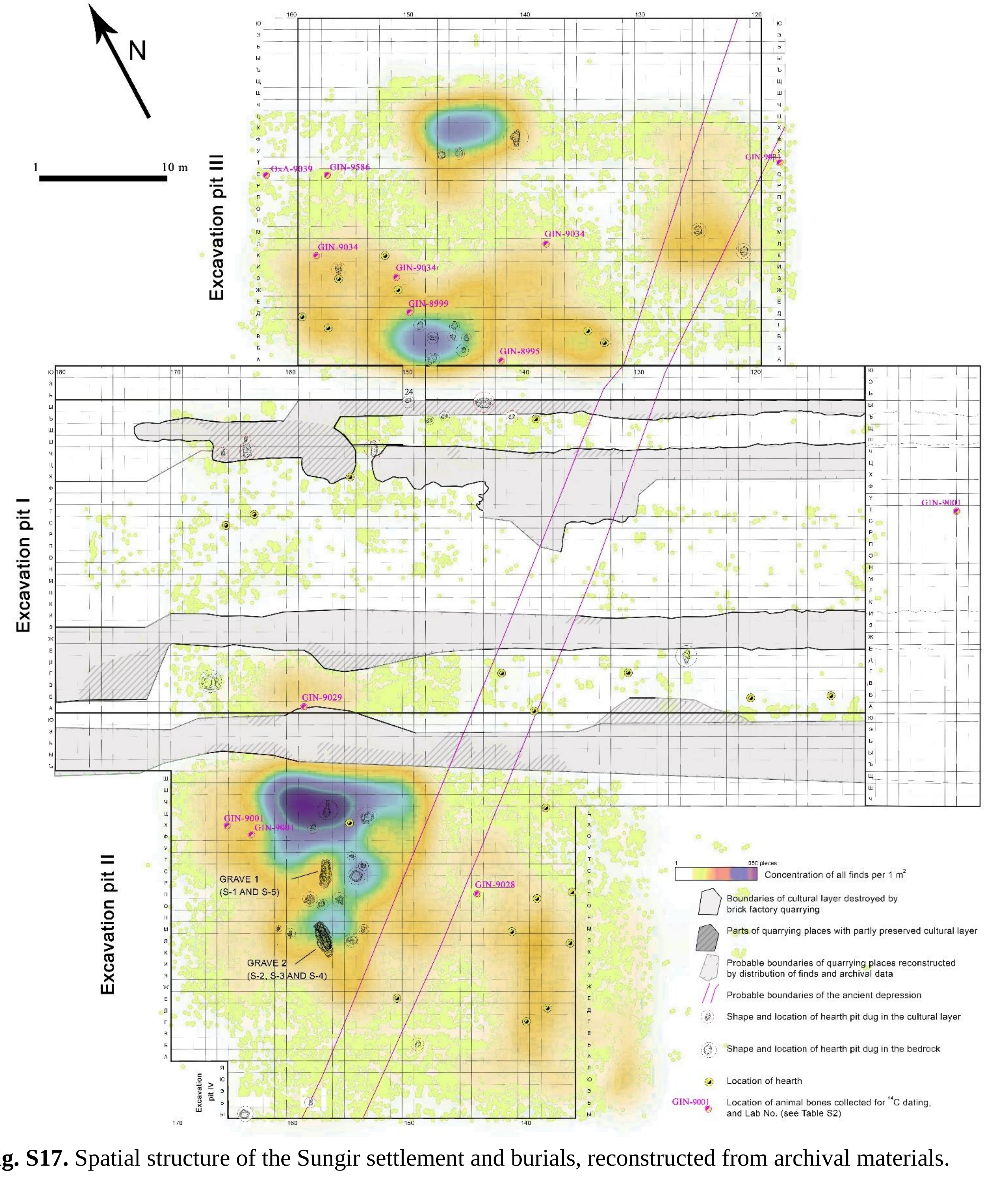

Fig. S17. Spatial structure of the Sungir settlement and burials, reconstructed from archival materials.

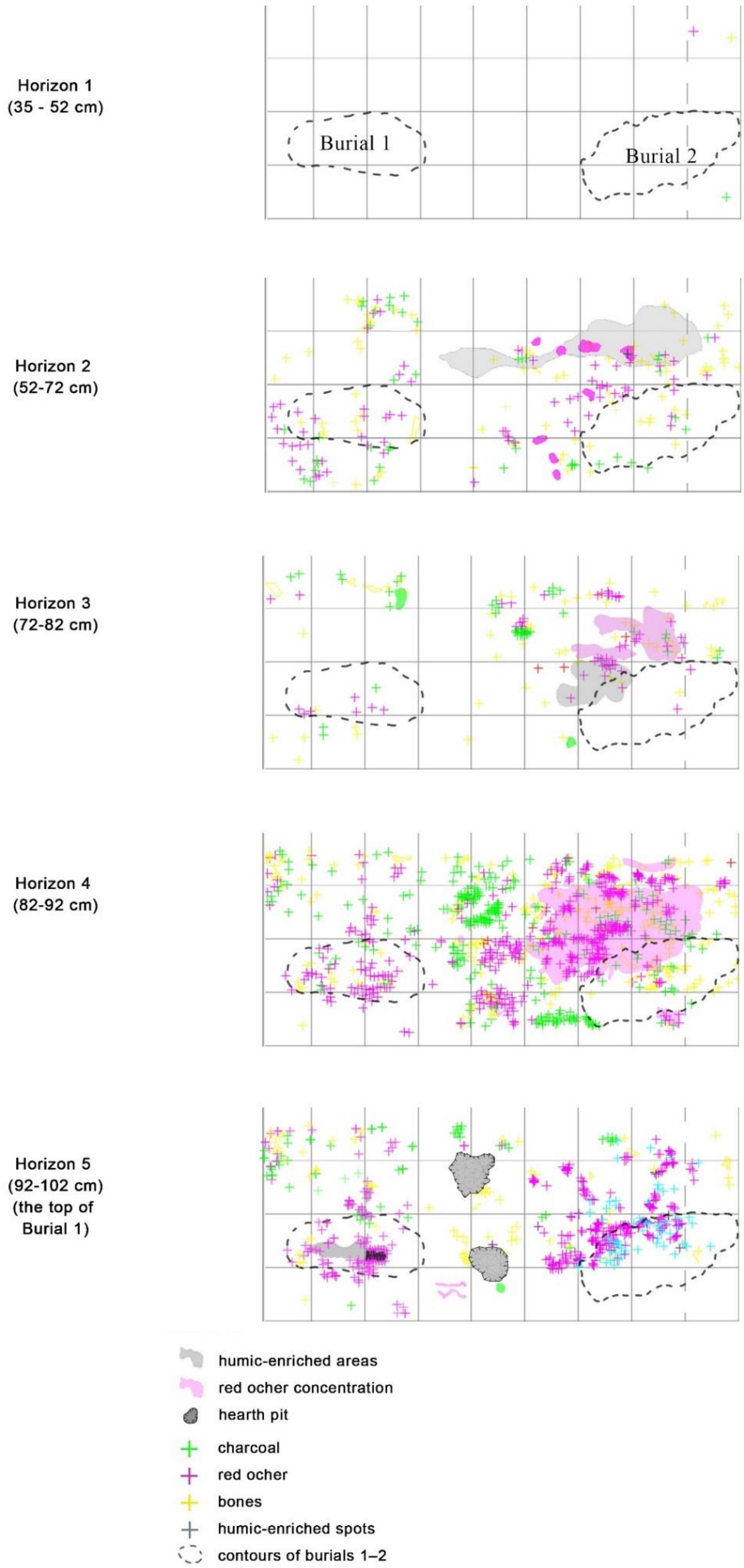

Fig. S18. Spatial structure of the part of Pit II above the burials, by 10 cm horizons, reconstructed from archival materials.

Table S1. ^{14}C dates on animal bones from the Sungir site (after Sulerzhitsky et al. 2000; Dobrovolskaya et al. 2012a; Trinkaus et al. 2015; Gavrilov et al. 2021; Stulova 2021; this paper). The material dated is non-ultrafiltered collagen, unless otherwise indicated.

Year, excavation pit, grid [a]	Species	Arbitrary level	^{14}C date, BP	Lab code	Calendar age, cal BP (95.4%) [b]	Relationship with burials
1963, Pit I, grid A/154	mammoth	?	20,360 ± 900	GIN-9585	22,530–26,320	unclear
1966, Pit I, grid M/164	mammoth	3	23,600 ± 600	GIN-8998	26,490–29,100	unclear
1958, Pit I, grids T/102–103; Pit II, grids KH-F-U [ХФУ]/163, 165, 166; KH-F-TS [ХФЦ]/163	horse [c]	?	25,770 ± 600	GIN-9001	28,900–31,090	unclear
1966, Pit III, grid ZH [Ж]/166; 1969, Pit III, grids Z [З]/151, K/158, L/138	horse [d]	3–4?	26,300 ± 300	GIN-9034	30,070–31,050	unclear
1961, Pit III, grid A/142	mammoth	3	26,300± 260	GIN-8995	30,090–31,030	unclear
1966, Pit III, grid B [Б]/164	mammoth	?	26,600 ± 300	GIN-9030	30,200–31,180	unclear
1969, Pit III, grid M/147	reindeer	1	26,600 ± 300	GIN-9035	30,200–31,180	unclear
1963, Pit I, grid ?	mammoth	?	27,000 ± 320	GIN-9591	30,430–31,670	unclear
1963, Pit I, grid ?	mammoth	?	27,200 ± 400	GIN-9027	30,430–31,970	unclear
1970, Pit III, grid S [С]/157	mammoth	3	27,200 ± 500	GIN-9586	30,200–32,750	unclear
1957, Pit II, grid line V [В] – ZH [Ж]	reindeer	?	27,260 ± 500	GIN-9036	30,300–33,100	unclear
1966, Pit I, grids A/127, S [С], T/147; Pit II, grids P [П]/132, S [С], T/159–160, TS [Ц]/147	horse [e]	?	27,400 ± 400	GIN-9033	30,810–32,790	unclear
1995, Pit III, grid S [С]/162	mammoth	4	27,460 ± 310	OxA-9039 [f]	31,050–32,010	below the burials
1995, Pit III, grid S [С]/162	mammoth	4	29,640 ± 180	OxA-15752 [f]	33,810–34,500	
1995, Pit III, grid S [С]/162	mammoth	4	29,450 ± 180	OxA-15755 [f]	33,580–34,410	
1995, Pit III, grid S [С]/162	mammoth	4	30,100 ± 400	OxA-X-2395-8 [f]	33,850–35,340	
1966, Pit III, grid T/118	mammoth	2	27,630 ± 280	GIN-9031	31,110–32,160	unclear
1987, Pit IIa, the surface of dark soil horizon	mammoth	?	27,700 ± 500	GIN-5880	31,000–33,150	unclear
1963, Pit I, grid V [В]/109	mammoth	?	27,800 ± 600	GIN-9588	30,950–33,600	unclear
1963, Pit I, grid P [П]/151	mammoth	?	28,000 ± 250	GIN-8997	31,380–32,930	unclear
1966, Pit I, grid A/159	mammoth	2	28,000± 300	GIN-9029	31,300–32,990	unclear
1967, Pit III, grid D [Д]/150	mammoth	3	28,120 ± 170	GIN-8999	31,690–32,900	unclear
1963, Pit I, grids L [Л]/132–133	mammoth	?	28,130 ± 370	GIN-8996	31,290–33,250	unclear
1966, Pit I, grids R, S [Р, С]/170	mammoth	1	28,350 ± 200	GIN-9032	31,850–33,140	unclear
1970, Pit II, grid P [П]/144	mammoth	3	28,800 ± 240	GIN-9028	32,190–33,910	below the burials [g]
2014, Test pit 4, depth -285 from the datum	reindeer	4 [h]	28,900 ± 330	OxA-30843 [i]	32,170–34,160	below the burials
2014, Test pit 4, depth -285/-295 from the datum	reindeer	4 [h]	29,650 ± 350	OxA-30844 [i]	33,290–34,710	below the burials
2014, Test pit 3, depth -339 from the datum	bone [j]	?	29,670 ± 350	OxA-30846 [i]	33,300–34,740	unclear, redeposited
2014, Test pit 4, depth -347 from the datum	bone [j]	5–6 [h]	30,140 ± 370	OxA-30842 [i]	33,980–35,330	below the burials
2014, Test pit 3, depth -333.5 from the datum	bone [j]	?	30,320 ± 380	OxA-30845 [i]	34,140–35,450	unclear, redeposited

[a] In square brackets, the original Russian letters are indicated if different from the English alphabet (see Sulerzhitsky et al. 2000).
[b] Calib Rev 8.1.0 software was used (Reimer et al. 2020). Calibrated ranges combined; values are rounded to the next 10 years.
[c] Seven bones; combined sample.

[d] Five bones; combined sample.
[e] Six bones; combined sample.
[f] These dates were run on the same bone, with non-ultrafiltered collagen (OxA-9039), ultrafiltered collagen (OxA-15752 and 15755) and hydroxyproline (OxA-X-2395-8) (Marom et al. 2012).
[g] This sample is the most securely associated with the layer below the burials (among the samples collected before 2015), in relative vicinity to them (see Figure S17).
[h] The correlation with arbitrary levels of ON Bader was obtained on the basis of Stulova (2021).
[i] Ultrafiltered collagen was dated.
[j] Unidentified to species.

Table S2. Stable isotope values for the Sungir humans and other Early Upper Paleolithic modern humans from Eastern and Central Europe.

Site, skeleton	$C:N_{atom}$ ratio	% C	% N	$\delta^{13}C$, ‰	$\delta^{15}N$, ‰	Collagen yield, %	Radiocarbon date, BP	Calendar age (cal B.P.), median value	Reference
Eastern Europe									
Sungir, S-1*	**3.3**	**29.64**	**10.60**	**-19.9**	**12.0**	**4.4**	26,100 ± 200	ca. 30,300	This paper
	—	—	—	-19.2	11.3	—	22,930 ± 200	ca. 27,570	Pettitt and Bader (2000)
	3.1	44.5	16.8	-19.5	10.7	—	27,050 ± 210	ca. 31,340	Dobrovolskaya et al. (2012a)
	3.2	40.2	14.8	-19.7	11.3	8.9	29,780 ± 420	ca. 34,240	This paper
Sungir, S-2*	**3.3**	**39.50**	**13.90**	**-19.5**	**11.6**	**15.1**	25,910 ± 130	ca. 30,150	This paper
	3.5	—	—	-19.0	11.2	6.0	23,830 ± 220	ca. 28,680	Pettitt and Bader (2000)
	3.1	—	—	-19.9	11.1	5.4	26,190 ± 120	ca. 30,880	Kuzmin et al. (2014)
	3.4	38.7	13.3	-20.1	11.3	15.5	25,630 ± 250	ca. 29,780	This paper
Sungir, S-3*	**3.3**	**31.40**	**11.10**	**-19.7**	**11.8**	**9.1**	26,780 ± 140	ca. 30,940	This paper
	3.4	—	—	-18.9	11.3	3.4	24,100 ± 240	ca. 28,930	Pettitt and Bader (2000)
	3.5	44.0	14.8	-19.6	11.0	—	26,000 ± 410	ca. 30,520	Dobrovolskaya et al. (2012a)
Sungir, S-5	3.4	34.9	—	-17.9	12.9	1.2	25,240 ± 160	ca. 29,280	Sikora et al. (2017)
Kostenki 14	3.1	—	—	-19.5	13.5	—	33,250 ± 500	ca. 37,840	Dobrovolskaya and Tiunov (2011)
Kostenki 1†	3.1	38.1	—	-18.3	15.3	6.6	32,070 ± 190	ca. 36,360	Higham et al. (2006)
Buran-Kaya III (BK3-07-01)	3.3	43.2	15.3	-19.4	15.4	—	31,900 ± 230	ca. 36,200	Prat et al. (2011)
Buran-Kaya III (BK3-11-01)	3.1	34.6	13.2	-18.8	15.8	—	—	—	Drucker et al. (2017)
Buran-Kaya III (BK3-12-01)	3.2	41.9	15.4	-18.9	16.8	—	—	—	Drucker et al. (2017)
Kostenki 8	3.2	—	—	-18.3	10.9	—	23,020 ± 320	ca. 27,180	Dobrovolskaya et al. (2012b)
Central Europe									
Peştera cu Oase 1	3.3	—	—	-19.0	13.3	4.0	34,920 ± 920	ca. 39,070	Trinkaus et al. (2009)
Peştera Muierii 1	3.4	41.5	13.3	-19.3	12.3	13.3	29,930 ± 170	ca. 34,030	Trinkaus et al. (2009)
Peştera Muierii 2	3.3	41.7	14.9	-19.1	12.4	11.2	29,110 ± 190	ca. 33,860	Trinkaus et al. (2009)
Peştera Cioclovina Uscată 1	3.4	44.4	15.9	-19.6	12.7	5.9	28,510 ± 170	ca. 32,430	Trinkaus et al. (2009)
Dolní Věstonice II, DV16	3.3	38.5	13.8	-19.7	12.5	13.9	27,220 ± 110	ca. 31,300	Fewlass et al. (2019)
Dolní Věstonice II, DV43	3.3	38.9	13.7	-19.6	12.6	10.2	27,070 ± 110	ca. 31,160	Fewlass et al. (2019)
Dolní Věstonice II, DV13	3.2	38.5	14.0	-19.3	12.9	13.5	27,040 ± 100	ca. 31,140	Fewlass et al. (2019)
Dolní Věstonice II, DV42	3.4	39.2	13.5	-19.8	12.7	9.0	26,880 ± 110	ca. 31,070	Fewlass et al. (2019)
Dolní Věstonice II, DV14	3.5	39.0	13.1	-20.2	13.3	9.5	26,760 ± 100	ca. 31,010	Fewlass et al. (2019)
Dolní Věstonice II, DV15	3.2	37.1	13.3	-19.4	12.6	8.0	26,680 ± 70	ca. 30,960	Fewlass et al. (2019)
Pavlov, Pav 1	3.4	41.2	14.3	-19.5	13.6	9.3	25,490 ± 90	ca. 29,690	Fewlass et al. (2019)
Brno-Francouzská 2	—	—	—	-19.0	12.3	—	23,680 ± 200	ca. 28,510	Trinkaus et al. (2009)
Dolní Věstonice 35	—	—	—	-18.8	12.3	—	22,840 ± 200	ca. 27,480	Trinkaus et al. (2009)
Předmostí 1	3.6	32.5	10.6	-19.4	12.6	2.6	—	—	Bocherens et al. (2015)

*The values in bold for the S-1 – S-3 individuals are used in this paper.
†Average values (see Richards et al. 2001; Higham et al. 2006).

References

Alekseeva TI, Bader NO, editors. 2000. Homo Sungirensis. Upper Palaeolithic man: ecological and evolutionary aspects of the investigation. Moscow: Nauchny Mir Press. In Russian with English summary.

Bader ON. 1978. Sungir. Verkhnepaleoliticheskaya stoyanka., Moscow: Nauka Publishers. In Russian.

Bader ON. 1998. Sungir. Paleolithic burials. In: Bader NO, Lavrushin YA, editors. The Upper Paleolithic site Sungir (graves and environment). Moscow: Nauchny Mir Press. p. 5–158. In Russian with English abstract.

Bader NO, Lavrushin YA, editors. 1998. The Upper Paleolithic site Sungir (graves and environment). Moscow: Nauchny Mir Press. In Russian with English abstract.

Bocherens H, Drucker DG, Germonpre M, Lázničková-Galetová ., Naito YI, Wissing C, Brůžek J, Oliva M. 2015. Reconstruction of the Gravettian food-web at Předmostí I using multi-isotopic tracking (^{13}C, ^{15}N, ^{34}S) of bone collagen. Quaternary International 359–360:211–228.

Dobrovolskaya MV, Tiunov AV. 2011. Stable isotope ($^{13}C/^{12}C$ and $^{15}N/^{14}N$) evidence for Late Pleistocene hominides' palaeodiets in Gorny Altai. In: Derevianko AP, Shunkov MV, editors. Characteristic features of the Middle to Upper Paleolithic transition in Eurasia., Novosibirsk: Institute of Archaeology and Ethnography Press. p. 81–89.

Dobrovolskaya M, Richards MP, Trinkaus E. 2012a. Direct radiocarbon dates for the mid Upper Paleolithic (eastern Gravettian) burials from Sunghir, Russia. Bulletin et Mémoires de la Societe d'Anthropologie de Paris 24(1–2):96–102.

Dobrovolskaya MV, Mednikova MB, Buzhilova AP, Tiunov, AV, Selezneva VI, Moiseev VG, Khartanovich VI. 2012b. Bioarchaeological study of human skeletal fragments from Upper Paleolithic site Kostenki 8. Kratkie Soobshcheniya Instituta Arkheologii RAN 227:103–112. In Russian with English abstract.

Drucker DG, Naito YI, Péan S, Prat S, Crépin L, Chikaraishi Y, Ohkouchi N, Puaud S, Lázničková-Galetová M, Patou-Mathis M, Yanevich A, Bocherens H. 2017. Isotopic analyses suggest mammoth and plant in the diet of the oldest anatomically modern humans from far southeast Europe. Scientific Reports 7:6833.

Fewlass H, Talamo S, Kromer B, Bard E, Tuna T, Fagault Y, Sponheimer M, Ryder C, Hublin J-J, Perri A, Sázelová S, Svoboda J. 2019. Direct radiocarbon dates of mid Upper Palaeolithic human remains from Dolní Věstonice II and Pavlov I, Czech Republic. Journal of Archaeological Science: Reports 27:102000.

Gavrilov KN. 2001. Arkheologichesky kontekst pogrebenyi Sungirya. In: Grigoryeva GV, editor. Kamenny vek Starogo Sveta. St. Petersburg: AkademPrint. p. 31–32. In Russian.

Gavrilov K. 2017. Sungir: The choice between Szeletian and Aurignacian. In: Vasil'ev S, Sinitsyn A, Otte M, editors. Le Sungirien (ERAUL, Etudes et Recherches Archéologiques de l'Université de Liège, vol. 147). Liège: Université de Liège. p. 107–117.

Gilligan I. 2019. Climate, clothing and agriculture in prehistory: linking evidence, causes, and effects. New York: Cambridge University Press.

Higham TFG, Jacobi RM, Bronk Ramsey C. 2006. AMS radiocarbon dating of ancient bone using ultrafiltration. Radiocarbon 48(2):179–195.

Kuzmin YV, Keates SG. 2014. Direct radiocarbon dating of Late Pleistocene hominids in Eurasia: current status, problems, and perspectives. Radiocarbon 56(2):753–766.

Kuzmin YV, van der Plicht J, Sulerzhitsky LD. 2014. Puzzling radiocarbon dates for the Upper Paleolithic site of Sungir (central Russian Plain). Radiocarbon 56(2):451–459.

Marom A, McCullagh JSO, Higham TFG, Sinitsyn AA, Hedges REM. 2012. Single amino acid radiocarbon dating of Upper Paleolithic modern humans. Proceedings of the National Academy of Science of the USA 109(18):6878–6881.

Pettitt PB, Bader NO. 2000. Direct AMS radiocarbon dates for the Sungir mid Upper Palaeolithic burials. Antiquity 74(284):269–270.

Prat S, Péan SC, Crépin L, Drucker DG, Puaud SJ, Valladas H, Lázničková-Galetová M, van der Plicht J, Yanevich A. 2011. The oldest anatomically modern humans from far southeast Europe: direct dating, culture and behavior. PLoS ONE 6(6):e20834.

Reimer PJ, Austin WEN, Bard E, Bayliss A, Blackwell PG, Bronk Ramsey C, Butzin M, Cheng H, Edwards RL, Friedrich M, Grootes PM, Guilderson TP, Hajdas I, Heaton TJ, Hogg AG, Hughen KA, Kromer B, Manning SW, Muscheler R, Palmer JG, Pearson C, van der Plicht J, Reimer RW, Richards DA, Scott EM, Southon JR, Turney CSM, Wacker L, Adolphi F, Büntgen U, Capano M, Fahrni SM, Fogtmann-Schulz A, Friedrich R, Köhler P, Kudsk S, Miyake F, Olsen J, Reinig F, Sakamoto M, Sookdeo A, Talamo S. 2020. The IntCal20 Northern Hemisphere radiocarbon age calibration curve (0–55 cal kBP). Radiocarbon 62(4):725–757.

Richards MP, Trinkaus E. 2009. Isotopic evidence for the diets of European Neanderthals and early modern humans. Proceedings of the National Academy of Science of the USA 106(38):16034–16039.

Richards MP, Pettitt PB, Stiner MC, Trinkaus E. 2001. Stable isotope evidence for increasing dietary breadth in the European mid-Upper Paleolithic. Proceedings of the National Academy of Science of the USA 98(11):6528–6532.

Sikora M, Seguin-Orlando A, Sousa VC, Albrechtsen A, Korneliussen T, Ko A, Rasmussen S, Dupanloup I, Nigst PR, Bosch MD, Renaud G, Allentoft ME, Margaryan A, Vasilyev SV, Veselovskaya EV, Borutskaya SB, Deviese T, Comeskey D, Higham T, Manica A, Foley R, Meltzer

DJ, Nielsen R, Excoffier L, Lahr MM, Orlando L, Willerslev E. 2017. Ancient genomes show social and reproductive behavior of early Upper Paleolithic foragers. Science 358(6363):659–662.

Sulerzhitsky LD, Pettitt P, Bader NO. 2000. Radiocarbon dates of the remains from the settlement Sunghir. In: Alekseeva TI, Bader NO, editors. Homo Sungirensis. Upper Palaeolithic man: ecological and evolutionary aspects of the investigation. Moscow: Nauchny Mir Press. p. 30–34. In Russian with English summary.

Trinkaus E, Soficaru A, Doboş A, Constantin S, Zilhão J, Richards M. 2009. Stable isotope evidence for early modern human diet in Southeastern Europe: Peştera cu Oase, Peştera Muierii and Peştera Cioclovina Uscată. Materiale si Cercetări Arheologice (serie nouă) V:5–14.

Trinkaus E, Buzhilova AP, Mednikova MB, Dobrovolskaya MV, editors. 2014. The people of Sunghir: burials, bodies, and behavior in the earlier Upper Paleolithic. New York: Oxford University Press.

Trinkaus E, Buzhilova AP, Mednikova MB, Dobrovolskaya MV. 2015. The age of the Sunghir Upper Paleolithic human burials. Anthropologie 53(1/2):221–231.

Vasilyev SV, Gerasimova MM. 2017. Historiographical review of comprehensive study of the Upper Paleolithic site Sungir on the Klyazma River and its dwellers (brief archaeological and paleoanthropological overview). In: Vasil’ev S, Sinitsyn A, Otte M, editors. Le Sungirien (ERAUL, Etudes et Recherches Archéologiques de l’Université de Liège, vol. 147). Liège: Université de Liège. p. 47–60.

Zhitenev VS. 2017. Personal ornaments and decorated objects from the Early Upper Paleolithic site of Sungir. In: Vasil’ev S, Sinitsyn A, Otte M, editors. Le Sungirien (ERAUL, Etudes et Recherches Archéologiques de l’Université de Liège, vol. 147). Liège: Université de Liège. p. 73–84.

Zubov AA, editor. 1984. Sungir: antropologicheskoe issledovanie. Moscow: Nauka Publishers. In Russian.